HHS Public Access

Author manuscript

J Clin Exp Oncol. Author manuscript; available in PMC 2015 August 11.

Published in final edited form as:

J Clin Exp Oncol. 2013 ; 2(2): .

Gemcitabine-(C_4-*amide*)-[anti-HER2/*neu*] Anti-Neoplastic Cytotoxicity in Dual Combination with Mebendazole against Chemotherapeutic-Resistant Mammary Adenocarcinoma

C.P. Coyne[1,*], **Toni Jones**[1], and **Ryan Bear**[2]

[1]Department of Basic Sciences (College of Veterinary Medicine), Mississippi State University, USA

[2]College of Veterinary Medicine at Wise Center, Mississippi State University, USA

Abstract

Introduction—Gemcitabine is a pyrimidine nucleoside analog that becomes triphosphorylated and competitively inhibits cytidine incorporation into DNA strands. Diphosphorylated gemcitabine irreversibly inhibits ribonucleotide reductase thereby preventing deoxyribonucleotide synthesis. Functioning as a potent chemotherapeutic, gemcitabine decreases neoplastic cell proliferation and induces apoptosis which accounts for its effectiveness in the clinical treatment of several leukemia and carcinoma cell types. A brief plasma half-life due to rapid deamination, chemotherapeutic-resistance and sequelae restrict gemcitabine utility in clinical oncology. Selective “targeted” gemcitabine delivery represents a molecular strategy for prolonging its plasma half-life and minimizing innocent tissue/organ exposure.

Methods—A previously described organic chemistry scheme was applied to synthesize a UV-photoactivated gemcitabine intermediate for production of gemcitabine-(C_4-*amide*)-[anti-HER2/*neu*]. Immunodetection analysis (Western-blot) was applied to detect the presence of any degradative fragmentation or polymerization. Detection of retained binding-avidity of gemcitabine-(C_4-*amide*)-[anti-HER2/*neu*] was determined by cell-ELISA using populations of chemotherapeutic-resistant mammary adenocarcinoma (SKBr-3) that highly over-express the HER2/*neu* trophic membrane receptor. Cytotoxic anti-neoplastic potency of gemcitabine-(C_4-*amide*)-[anti-HER2/*neu*] and the benzimidazole tubulin/microtubule inhibitors, albendazole, flubendazole and mebendazole was established against chemotherapeutic-resistant mammary adenocarcinoma (SKBr-3). Related investigations evaluated the potential for gemcitabine-(C_4-*amide*)-[anti-HER2/*neu*] in dual combination with mebendazole to evoke increased levels of cytotoxic anti-neoplatic potency compared to gemcitabine-(C_4-*amide*)-[anti-HER2/*neu*].

Results—Covalent gemcitabine-(C_4-*amide*)-[anti-HER2/neu] immunochemotherapeutic and each benzimidazole (n=3) exerted cytotoxic anti-neoplastic potency against chemotherapeutic-resistant mammary adenocarcinoma (SKBr-3). Covalent gemcitabine-(C_4-*amide*)-[anti-HER2/

[*]Corresponding author: C.P. Coyne, Department of Basic Sciences (College of Veterinary Medicine), Mississippi State University, Mississippi State, Mississippi 39762, USA, Tel: 662 325-1120; coyne@cvm.msstate.edu.

Conflict of Interest: Source of Research Support: residual extramural funding from the conduction of a previous un-related research investigation.

neu] immunochemotherapeutic or gemcitabine in dual combination with mebendazole created increased levels of cytotoxic anti-neoplastic potency that were greater than attained with gemcitabine-(C_4-*amide*)-[anti-HER2/*neu*] or gemcitabine alone.

Conclusion—Gemcitabine-(C_4-*amide*)-[anti-HER2/*neu*] in dual combination with benzimidazoles can produce enhanced levels of cytotoxic anti-neoplastic activity and potentially provide a basis for treatment regimens with a wider margin-of-safety. Such benefits would be possible through the collective properties of; [*i*] selective "*targeted*" gemcitabine delivery; [*ii*] relatively lower toxicity of benzimidazoles compared to many if not most conventional chemotherapeutics; [*iii*] reduced total dosage requirements faciliated by additive or synergistic anti-cancer properties; and [*iv*] differences in sequelae for gemcitabine-(C_4-*amide*)-[anti-HER2/*neu*] compared to benzimidazole tubulin/microtubule inhibitors.

Keywords

Anti-HER2/neu; Benzimidazoles; Chemotherapeutic-resistant; Covalent immunochemotherapeutic; Cytotoxic anti-neoplastic potency; Dual combination anti-cancer therapy; Gemcitabine-(C4-amide)-[anti-HER2/neu]; Mammary adenocarcinoma

Introduction

Monoclonal immunoglobulin preparations or pharmaceuticals with binding-avidity for HER2/*neu* (e.g. anti-HER2/*neu*: trastuzumab, pertuzumab) [1-5] EGFR (e.g. anti-EGFR: cetuximab, gefitinib) [6-9] immunoglobulin fractions with dual binding-avidity for both HER2/neu and EGFR (e.g. anti-HER2/*neu* and anti-EGFR properties: panitumumab) [8-11] or monoclonal immunoglobulin inhibitors of other trophic receptors can all be effective treatment options for cancer including forms affecting the breast, intestinal tract, lung and prostate. The obvious advantage of these preparations is their ability to function as an anti-cancer treatment modality that avoids many of the sequelae associated with conventional chemotherapeutics. Unfortunately, most monoclonal immunoglobulin-based therapies that inhibit trophic membrane receptor function are usually only capable of promoting cytostatic properties and are almost invariably plagued by an inability to evoke cytotoxic activity sufficient to effectively resolve most aggressive or advanced forms of neoplastic disease [12-17].

The anthracyclines have traditionally been the class of chemotherapeutics most commonly bonded covalently to (large) molecular platforms that can facilitate "selective" targeted delivery. Gemcitabine, in contrast to the anthracyclines, is a chemotherapeutic that has less frequently been covalently bound to large molecular weight platforms that can provide various biological properties [18,19] including selective "targeted" delivery [20] Gemcitabine is a deoxycytidine nucleotide analog with a mechanism-of-action that is dependent upon intracellular triphosphoralation which allows it to substitute for cytidine during DNA transcription. In this capacity triphosphoralated gemcitabine both inhibits DNA polymerase biochemical activity and is incorporated into DNA strands. A second mechanism-of-action involves gemcitabine inhibiting and inactivating ribonucleotide reductase in concert with suppression of deoxyribonucleotide synthesis, diminished DNA repair and declines in DNA transcription. Each of these mechanisms-of-action induces the

onset of apoptosis. In clinical oncology, gemcitabine is administered for the treatment of certain leukemias and potentially diferent types of lymphoma in addition to a spectrum of adenocarcinomas and carcinomas affecting the lung (e.g. non-small cell), pancrease, bladder and esophogus. The plasma half-life for gemcitabine is brief because it is rapidly deaminated to an inactive metabolite that is then redily eliminated through renal excretion into the urine [21-23].

Several distinct attributes can be realized through the molecular design and organic chemistry synthesis of a covalent gemcitabine immunochemotherapeutic that in part include the properties of selective “targeted” chemotherapeutic delivery, continual deposition, progressive intracellular accumulation, and extended plasma gemcitabine pharmacokinetic profile. Presumably due steric hinderance phenomenon, gemcitabine covalently bound to large molecular weight platforms like immunoglobulin is less vulnerable to MDR-1 (multi-drug resistance efflux pump) [24], or biochemical deamination by cytidine deaminase and deoxycytidylate deaminase (following gemcitabine phosphorylation). Complementary advantages of covalently bonding gemcitabine to immunoglobulin or molecular ligands are the obvious opportunity they afford to evoke additive or synergistic levels of cytotoxic anti-neoplastic potency. In this regard, anti-HER2/*neu*, anti-EGFR and similar monoclonal immunoglobulin fractions provide a mechanism for simultaneously achieving selective “targeted” chemotherapeutic delivery and suppression of neoplastic cell biological vitality in populations that are heavily dependent on trophic receptor over-expression.

Gemcitabine in clinical scenarios is frequently administered in combination with tubulin/microtubule inhibitor chemotherapeutics including the vinca alkaloids [25-28] taxanes [28-30] podophyllotoxins/etoposides [31-33] and monomethyl auristatin E (MMAE) [34]. Such combinations have commonly been administered for the therapeutic management of neoplastic conditions affecting the breast [25-28,29] pancrease [33] lung [31] in addition to lymphoproliferative disorders [34]. Clinical trials have been conducted to evaluate the efficacy of gemcitabine in combination with vinca alkaloid (2010: sarcomas) and Brentuximab Vedotin (2011: anaplastic large cell lymphoma and Hodgkin's Lymphoma). The benzimidazole anthelmintic agents functionally have a mechanism-of-action highly analogous to the vinca alkaloids and other tubulin/microtubule inhibitor chemotherapeutics. Given this perspective, benzimidazoles individually and mebendazole in dual combination with covalent gemcitabine-(C_4-*amide*)-[anti-HER2/*neu*] immunochemotherapeutic were accessed for their individual and combined cytotoxic anti-neoplastic potency against chemotherapeutic-resistant mammary adenocarcinoma (SKBr-3) due to their potential for achieving additive or synergistic levels of efficacy.

Materials and Methods

Synthesis of covalent Gemcitabine-(C_4-*amide*)-[anti-HER2/*neu*] Immunochemotherapeutic

Phase-I Synthesis Scheme for UV-Photoactivated Gemcitabine-(C_4-amide) Intermediate—Te cytosine-like C_4-amine of gemcitabine (0.738 mg, 2.80×10^3 mmoles) was reacted at a 2.5:1 molar-ratio with the amine-reactive *N*-hydroxysuccinimide ester “leaving” complex of succinimidyl 4,4-azipentanoate (0.252 mg, 1.12×10^{-3} mmoles) in the presence of triethylamine (TEA 50 mM final concentration) utilizing dimethylsulfoxide as

an organic solvent system (Figure 1). The reaction mixture of gemcitabine and succinimidyl 4,4-azipentanoate was continually stirred at 25° C for 4-hours in the dark.

Phase-II Synthesis Scheme for Covalent Gemcitabine-(C_4-amide)-[anti-HER2/neu] Immunochemotherapeutic Utilizing a UV-Photoactivated Gemcitabine Intermediate—Immunoglobulin fractions of anti-HER2/*neu* (1.5 mg, 1.0×10^{-5} mmoles) in buffer (PBS: phosphate 0.1, NaCl 0.15 M, EDTA 10 mM, pH 7.3) were combined at a 1:10 molar-ratio with the UV-photoactivated gemcitabine-(C_4-*amide*) intermediate (*Phase-1 end product*) and allowed to gently mix by constant stirring for 5 minutes at 25°C in the dark. The photoactivated group of the gemcitabine-(C_4-*amide*) intermediate was reacted with side chains of amino acid residues within the sequence of anti-HER2/*neu* monoclonal immunoglobulin during a 15 minute exposure to UV light at 354 nm (reagent activation range 320-370 nm) in combination with constant gentle stirring (Figure 1). Residual gemcitabine was removed from gemcitabine-(C_4-*amide*)-[anti-HER2/*neu*] applying micro-scale column chromatography following pre-equilibration of exchange media with PBS (phosphate 0.1, NaCl 0.15 M, pH 7.3).

Analytical characterization

General analyses—Approximation of the amount of non-covalently bound gemcitabine contained within the covalent gemcitabine-(C_4-*amide*)-[anti-HER2/*neu*] immunochemotherapeutic following separation by column chromatography was determined by measuring absorbance at 265-267 nm [35,36] of the resulting supernatant after precipitation of gemcitabine-immunochemotherapeutics with either chloroform [37-39] or methanol:acetonitrile (1:9 v/v) with measurements compared to original known concentrations [40]. Determination of the immunoglobulin concentration for the covalent gemcitabine-(C_4-*amide*)-[anti-HER2/*neu*] immunoconjugates was determined by measuring absorbance at 280 nm in combinations with utilizing a 235 nm -vs- 280 nm standardized reference curve in order to accommodate for any potential absorption profile over-lap at 280 nm between gemcitabine and immunoglobulin [20,40-44].

Molecular mass/size-dependent separation by non-reducing SDS-PAGE—Te covalent gemcitabine-(C_4-*amide*)-[anti-HER2/*neu*] immunochemotherapeutic and anti-HER2/*neu* immunoglobulin reference control were adjusted to a standardized protein concentration of 60 μg/ml and then combined 50/50 v/v with conventional SDS-PAGE sample preparation buffer (Tris/glycerol/bromphenyl blue/SDS) formulated without 2-mercaptoethanol or boiling. Each covalent immunochemotherapeutic, the reference control immunoglobulin fraction (0.9 μg/well) and a mixture of pre-stained reference control molecular weight markers were then developed by SDS-PAGE (11% acrylamide) at 100 V constant voltage at 3°C for 2.5 hours.

Western-blot immunodetection—Covalent gemcitabine-(C_4-*amide*)-[anti-HER2/*neu*] immunochemotherapeutic following SDS-PAGE was equilibrated in tank buffer devoid of methanol. Mass/size-separated gemcitabine anti-HER2/*neu* immunochemotherapeutic contained in acrylamide SDS-PAGE gels was then transferred laterally onto nitrocellulose membrane at 20 volts (constant voltage) for 16 hours at 2° to 3°C with the transfer manifold

packed in crushed ice. Nitrocellulose membranes with laterally-transferred immunochemotherapeutics were then equilibrated in Tris buffered saline (TBS: Tris HCl 0.1 M, NaCl 150 mM, pH 7.5, 40 ml) at 4°C for minutes followed by incubation in TBS blocking buffer solution (Tris 0.1 M, pH 7.4, 40 ml) containing bovine serum albumin (5%) for hours at 2° to 3°C applied in combination with gentle horizontal agitation. Prior to further processing, nitrocellulose membranes were vigorously rinsed in Tris buffered saline (Tris 0.1 M, pH 7.4, 40 ml, n=3×).

Rinsed BSA-blocked nitrocellulose membranes developed for Western-blot (immunodetection) analyses were incubated with biotinylated goat anti-murine IgG (1:10,000 dilution) at 4°C for 18 hours applied in combination with gentle horizontal agitation. Nitrocellulose membranes were then vigorously rinsed in TBS (pH 7.4, 4°C, 50 ml, n=3) followed by incubation in blocking buffer (Tris 0.1 M, pH 7.4, with BSA 5%, 40 ml). Blocking buffer was decanted from nitrocellulose membrane blots and then rinsed in TBS (pH 7.4, 4°C, 50 ml, n=3) before incubation with either strepavidin-HRPO (1:100,000 dilution) at 4°C for 2 hours applied in combination with gentle horizontal agitation. Prior to chemiluminescent development nitrocellulose membranes were vigorously rinsed in Tris buffered saline (Tris 0.1 M, pH 7.4, 40 ml, n=3). Development of nitrocellulose membranes by chemiluminescent autoradiography following processing with conjugated HRPO-strepavidin required incubation in HRPO chemiluminescent substrate (25°C; 5 to 10 mins.). Autoradiographic images were acquired by exposing radiographic film (Kodak BioMax XAR) to nitrocellulose membranes sealed in transparent ultraclear re-sealable plastic bags.

Mammary adenocarcinoma tissue culture—Chemotherapeutic-resistant human mammary adenocarcinoma (SKBr-3) was utilized as an *ex-vivo* neoplasia model. Mammary adenocarcinoma (SKBr-3) characteristically over-expresses epidermal growth factor receptor 1 (EGFR, ErbB-1, HER1) and highly over-expresses epidermal growth factor receptor 2 (EGFR2, HER2/*neu*, ErbB-2, CD340, p185) at 2.2×10^5/cell and 1×10^6/cell respectively. Mammary adenocarcinoma (SKBr-3) was propagated at >85% confluency in 150-cc^2 tissue culture flasks containing McCoy's 5a Modified Medium supplemented with fetal bovine serum (10% v/v) and penicillin-streptomycin at a temperature of 37°C under a gas atmosphere of air (95%) and carbon dioxide (CO_2 5%).

Cell-ELISA total membrane-bound immunoglobulin assay—Mammary adenocarcinoma (SKBr-3) suspensions were seeded into 96-well microtiter plates in aliquots of 2×10^5 cells/well and allowed to form an adherent monolayer over a period of 48 hours. The growth media contents of individual wells were then removed manually by pipette and serially rinsed (n=3) with PBS followed by stabilization of adherent cellular monolayers onto the plastic surface of 96-well plates with paraformaldehyde (4% in PBS, 15 minutes). Stabilized monolayers were then incubated with gemcitabine-(C_4-*amide*)-[anti-HER2/*neu*] immunoconjugates formulated at gradient concentrations of 0.1, 0.25, 0.5, 1.0, 5.0 and 10 μg/ml IgG/ml in tissue culture growth media (200 μl/well). Gemcitabine-(C_4-*amide*)-[anti-HER2/*neu*] was incubated in direct contact with mammary adenocarcinoma at 37°C for 3-hours under a gas atmosphere of air (95%) and carbon dioxide (CO_2 5%). Following serial rinsings with PBS (n=3), development of stabilized mammary adenocarcinoma (SKBr-3)

monolayers entailed incubation with β-galactosidase conjugated goat anti-mouse IgG (1:500 dilution) for 2 hours at 25°C with residual unbound immunoglobulin removed by serial rinsing with PBS (n=3). Final cell ELISA development required serial rinsing (n=3) of stabilized mammary adenocarcinoma (SKBr-3) monolayer populations with PBS followed by incubation with nitrophenyl-β-D-galactopyranoside substrate (100 μl/well of ONPG formulated fresh at 0.9 mg/ml in PBS pH 7.2 containing $MgCl_2$ 10 mM, and 2-mercaptoethanol 0.1 M). Absorbance within each individual well was measured at 410 nm (630 nm reference wavelength) after incubation at 37°C for a period of 15 minutes.

Cell vitality stain assay for anti-neoplastic cytotoxicity—Co-valent gemcitabine-(C_4-*amide*)-[anti-HER2/*neu*] immunochemo-therapeutic was formulated in growth media at chemotherapeutic-equivalent concentrations of 10^{-10}, 10^{-9}, 10^{-8}, 10^{-7}, and 10^{-6} M. Similarly, albendazole, flubendazole and mebendazole were individually formulated in growth media at benzimidazole-equivalent concentrations of 0.05, 0.1, 0.2, 0.3, 0.4, 0.5, 0.75, 1.0, 2.0 and 2.5 μM. The covalent immunochemotherapeutic or individual benzimidazole was then transferred in triplicate into 96-well microtiter plates containing mammary adenocarcinoma (SKBr-3) monolayers (growth media 200 μl/well) and allowed to incubate in direct contact with cell populations for either 72 or 182-hours (37°C under a gas atmosphere of air 95% and carbon dioxide/CO_2 5%). Incubation periods of greater than 96-hours required replenishing mammary adenocarcinoma (SKBr-3) populations with fresh tissue culture media formulated with or without covalent gemcitabine-immunochemotherapeutics or benzimidazole tubulin/microtubule inhibitors as indicated.

Cytotoxic potency of gemcitabine-(C_4-*amide*)-[anti-HER2/*neu*] or the benzimidazoles was measured by removing all contents within the 96-well microtiter plates manually by pipette followed by serial rinsing of monolayers (n=3) with PBS and and then incubated with 3-[4,5-dimethylthiazol-2-yl]-2,5-diphenyl tetrazolium bromide formulated in RPMI-1640 growth media devoid of pH indicator or bovine fetal calf serum (MTT: 5 mg/ml). During a 3-to-4 hour incubation period at 37°C under a gas atmosphere of air (95%) and carbon dioxide (5% CO_2) the enzyme mitochondrial succinate dehydrogenase was allowed to convert MTT vitality stain reagent to navy-blue formazone crystals within the cytosol of mammary adenocarcinoma (SKBr-3) populations (some reports suggest that NADH/NADPH-dependent cellular oxidoreductase enzymes may also be involved in the conversion process). Contents of the 96-well microtiter plate were then removed and the stabilized monolayers serially rinsed with PBS (n=3). The resulting blue intracellular formazone crystals were dissolved with DMSO (300 μl/well) and then spectrophotometric absorbance of the blue-colored supernantant measured at 570 nm using a computer integrated microtiter plate reader.

Results

Molar-incorporation-index

Size-separation of gemcitabine-(C_4-*amide*)-[anti-HER2/*neu*] by micro-scale column chromatography consistently yielded a covalent immunochemotherapeutic preparation that contained <4.0% of residual non-covalently bound chemotherapeutic [20,40-44]. Small

residual amounts of non-covalently bound chemotherapeutic remaining within covalent immunochemotherapeutic preparations is generally accepted to not be available for further removal through additional column chromatography separations [45] which closely correlates with results from previous investigations devoted to the molecular design and organic chemistry synthesis of similar covalent immunochemotherapeutics (unpublished data) [9,40-44]. Calculations estimated a 2.78 molar-incorporation index for covalent gemcitabine-(C_4-*amide*)-[anti-HER2/*neu*] immunochemotherapeutic.

Molecular weight profile analysis

Mass/size separation of covalent gemcitabine-(C_4-*amide*)-[anti-HER2/*neu*] immunochemotherapeutic by SDS-PAGE in combination with immunodetection analysis (Western blot) and chemiluminescent autoradiography recognized a single primary condensed band of 150-kDa between a molecular weight range of 5.0-kDa to 450-kDa (Figure 2). Patterns of low-molecular-weight fragmentation from hydrolytic or enzymatic degradation, or evidence of large-molecular weight polymerization of immunoglobulin fractions were not detected (Figure 2). The observed molecular weight of 150-kDa for gemcitabine-(C_4-*amide*)-[anti-HER2/*neu*] directly corresponds with the known molecular weight/mass of reference control anti-HER2/*neu* monoclonal immunoglobulin fractions (Figure 2). Analogous results have been reported for similar covalent immunochemotherapeutics [40-44,46,47].

Cell-binding analysis

Total cell-bound immunoglobulin in the form of gemcitabine-(C_4-*amide*)-[anti-HER2/*neu*] on the external surface membrane of adherent mammary adenocarcinoma (SKBr-3) populations was measured by cell-ELISA (Figure 3). Greater total membrane-bound gemcitabine-(C_4-*amide*)-[anti-HER2/*neu*] was detected with progressive increases in standardized total immunoglobulin-equivalent concentrations formulated at 0.010, 0.025, 0.050, 0.250, and 0.500 μg IgG/ml (Figure 3). The cell-ELISA profiles served to validate the retained selective binding-avidity of gemcitabine-(C_4-*amide*)-[anti-HER2/*neu*] for HER2/*neu* receptor sites highly over-expressed at 1×10^6/cell on the exterior surface membrane of mammary adenocarcinoma (SKBr-3) populations (Figure 3) [20].

Cytotoxic anti-neoplastic potency analysis

Gemcitabine-(C_4-*amide*)-[anti-HER2/*neu*] exerted a 41.1% maximum level of selective "targeted" cytotoxic anti-neoplastic potency (58.9% residual survival) against chemotherapeutic-resistant mammary adenocarcinoma (SKBr-3) at a gemcitabine-equivalent concentration of 10^{-6} M with progressive increases from 14% to 41.1% (86.0% and 58.9% residual survival) detected between 10^{-8} M and 10^{-6} M respectively over a direct-contact incubation period of 182-hours (Figure 4).

Cytotoxic anti-neoplastic potency profiles for gemcitabine-(C_4-*amide*)-[anti-HER2/*neu*] after a 182-hour direct-contact incubation period were highly analogous to gemcitabine chemotherapeutic following a 72-hour direct-contact incubation period at the gemcitabine-equivalent concentrations of 10^{-10}, 10^{-9}, 10^{-8}, 10^{-7} and 10^{-6} M (Figure 4). Gemcitabine alone at 182-hours produced rapid increases in cytotoxic anti-neoplastic potency from 5.8% to

88.3% (94.2% and 11.7% residual survival) at and between the gemcitabine-equivalent concentrations of 10^{-9} M and 10^{-7} M respectively (Figure 4). Maximum cytotoxic anti-neoplastic potency for gemcitabine was 92.5% (7.5% residual survival) at the gemcitabine-equivalent concentration of 10^{-6} M (Figure 4). Cytotoxic anti-neoplastic potency for gemcitabine-(C_4-*amide*)-[anti-HER2/*neu*] was detectably lower based on observed values of 27.3% and 40.1% (72.7% and 58.9% residual survival) at 10^{-7} M and 10^{-6} M respectively (Figure 4) [20]. Monoclonal anti-HER2/*neu* immunoglobulin fractions alone did not exert detectable levels of *ex-vivo* cytotoxic anti-neoplastic potency against chemotherapeutic-resistant mammary adenocarcinoma (SKBr-3) which is in direct accord with descriptions from previous investigations for anti-HER2/neu [40-44,47-51] and anti-EGFR [44] at 0-to-182 hours in populations of several diferent neoplastic cell types (Figure 4).

Te benzimadazole tubulin/microtubule inhibitors, albendazole, flubendazole and mebendazole exerted substantial cytotoxic antineoplastic potency against chemotherapeutic-resistant mammary adenocarcinoma (SKBr-3) over direct-contact incubation periods of both 72-hours and 182-hours when formulated in triplicate at final concentrations ranging between 0.05 μM to 2.5 μM (Figures 5-7). The benzimidazoles, flubendazole and mebendazole exerted near maximum levels of cytotoxic anti-neoplastic potencies of 70.2% and 63.1% (29.8% and 36.8% residual survival) at the final concentration of 0.4 μM in contrast to albendazole which reached only a level of 6.2% (93.8% residual survival at this same benzimidazole-equivalent concentration (Figure 6). Flubendazole produced a rapid increase in cytotoxic anti-neoplastic activity from 0.0% to 70.2% (100.0% and 29.8% residual survival) at and between the benzimidazole-equivalent concentrations of 0.05 μM and 0.4 μM while mebendazole produced rapid increases in cytotoxic anti-neoplastic activity from 0.1% to 63.1% (99.9% and 36.9% residual survival) at and between the same benzimidazole-equivalent concentrations of 0.05 μM and 0.5 μM respectively (Figure 6). In marked contrast, albendazole produced progressive increases in cytotoxic anti-neoplastic activity from 6.2% to 65.4% (93.8% and 34.6% residual survival) at and between the final concentrations of 0.4 μM and 2.0 μM respectively (Figure 6).

Following an incubation period of 182-hours, flubendazole and mebendazole exerted mean cytotoxic anti-neoplastic potencies of 14.5% and 12.2% (85.5% and 87.8% residual survival) which rapidly increased to near maximum levels of 90.8% and 83.9% (9.24% and 16.1% residual survival) at and between the final benzimidazole-equivalent concentrations of 0.10 μM and 0.3 μM respectively (Figure 7). In contrast, the mean cytotoxic anti-neoplastic potency for albendazole first progressively and then rapidly increased from 9.8% to 91.0% (90.2% and 9.0% residual survival) at and between the final benzimidazole-equivalent concentrations of 0.4 μM and 2.0 μM respectively (Figure 7). Albendazole, flubendazole and mebendazole all produced maximum levels of cytotoxic anti-neoplastic potencies of 91.0%, 90.8% and 91.2% (9.0%, 9.2% and 8.8% residual survival) at the final benzimidazole-equivalent concentration of 2.0 μM respectively (Figure 7). Increased duration of challenge (direct contact incubation) for the benzimidazoles with chemotherapeutic-resistant mammary adenocarcinoma (SKBr-3) populations resulted in detectably larger increases in anti-neoplastic cytotoxicity (Figures 6-8).

Te cytotoxic anti-neoplastic potency of gemcitabine-(C_4-*amide*)-[anti-HER2/*neu*] was markedly increased when chemotherapeutic-resistant mammary adenocarcinoma (SKBr-3) populations were challenged with the covalent immunochemotherapeutic in dual combination with mebendazole (0.15 μM fixed-concentration) at and between the gemcitabine-equivalent concentrations of 10^{-9} M and 10^{-6} M (Figures 9 and 10). Gemcitabine-(C_4-*amide*)-[anti-HER2/*neu*] in dual combination with mebendazole (0.15 μM fixed final concentration) compared to gemcitabine-(C_4-*amide*)-[anti-HER2/*neu*] alone each produced progressive and relatively rapid increases in cytotoxic anti-neoplastic potency from 24.2% and 10.2% (75.8% and 89.8% residual survival) to maximum levels of 68.8% and 41.1% (31.2% and 58.9% residual survival) at and between the gemcitabine-equivalent concentrations of 10^{-9} M and 10^{-6} M respectively (Figure 9). The cytotoxic anti-neoplastic potency profiles for gemcitabine-(C_4-*amide*)-[anti-HER2/*neu*] compared to gemcitabine alone where substantially different when they were each applied in dual combination with mebendazole (0.15 μM fixed-concentration) between the gemcitabine-equivalent concentrations of 10^{-9} to 10^{-6} M (Figures 9 and 10). Gemcitabine-(C_4-*amide*)-[anti-HER2/*neu*] in dual combination with mebendazole (0.15 μM fixed-concentration) produced progressive increases in cytotoxic anti-neoplastic potency from 24.2% to a maximum of 68.8% (75.8% and 31.2% residual survival) between the gemcitabine-equivalent concentrations of 10^{-9} M and 10^{-6} M respectively (Figures 9 and 10). Conversely, gemcitabine in dual combination with mebendazole (0.15 μM fixed-concentration) produced a rapid increase in cytotoxic anti-neoplastic potency from 33.2% to a maximum of 88.2% (66.8% and 11.8% residual survival) at the gemcitabine-equivalent concentrations of 10^{-9} M and 10^{-8} M respectively (Figures 9 and 10). Gemcitabine with mebendazole was much more potent than gemcitabine-(C_4-*amide*)-[anti-HER2/*neu*] with mebendazole at gemcitabine-equivalent concentrations of 10^{-8} and 10^{-7} M producing cytotoxic anti-neoplastic potency levels of 88.2% and 90.1% (11.8% and 9.9% residual survival) compared to 32.4% and 50.8.2% (67.6% and 49.2% residual survival) at the gemcitabine-equivalent concentrations of 10^{-8} M and 10^{-7} M respectively (Figure 10). Mean maximum cytotoxic anti-neoplastic potencies for gemcitabine-(C_4-*amide*)-[anti-HER2/*neu*] with mebendazole compared to gemcitabine with mebendazole were 68.8% and 88.7% (31.2% and 11.3% residual survival) respectively at the gemcitabine-equivalent concentration of 10^{-6} M (Figure 10).

Gemcitabine-(C_4-*amide*)-[anti-HER2/*neu*] in dual combination with mebendazole (0.15 μM fixed-concentration) produced greater levels of cytotoxic anti-neoplastic potency compared to gemcitabine alone at gemcitabine-equivalent concentrations of 10^{-10} M and 10^{-9} M, nearly equivalent levels at 10^{-8} M but lower levels at 10^{-7} M and 10^{-6} M respectively (Figure 10). Cytotoxic anti-neoplastic potency of gemcitabine-(C_4-*amide*)-[anti-HER2/*neu*] in dual combination with mebendazole (0.15 μM fixed-concentration) progressively increased from 24.2% to 61.8% (75.8% to 31.2% residual survival) at and between the gemcitabine-equivalent concentrations of 10^{-9} and 10^{-6} M (Figure 10). In contrast, gemcitabine alone produced rapid increases in cytotoxic anti-neoplastic potency from 5.8% to 88.3% (94.2% to 11.7% residual survival) between the gemcitabine-equivalent concentrations of 10^{-9} M and 10^{7} M respectively (Figure 10). Compared to gemcitabine-(C_4-*amide*)-[anti-HER2/*neu*] in dual combination with mebendazole (0.15 μM fixed-concentration), gemcitabine alone had greater cytotoxic anti-neoplastic potencies of 88.3%

versus 50.8% (11.7% and 49.2% residual survival) and maximum levels of 92.5% versus 68.8% (7.5% and 31.2% residual survival) at the gemcitabine-equivalent concentrations of 10^{-7} M and 10^{-6} M respectively (Figure 10).

Gemcitabine in dual combination with mebendazole (0.15 μM fixed-concentration) had a cytotoxic anti-neoplastic potency profile that was distinctly greater than detected for gemcitabine alone at the gemcitabine-equivalent concentrations of 10^{-10} M, 10^{-9} M and 10^{-8} M but not at 10^{-7} M or 10^{-6} M (Figure 10). Gemcitabine in dual combination with mebendazole (0.15 μM fixed-concentration) produced progressive and then rapid increases in cytotoxic antineoplastic potency from 30.3% to 88.2% (69.7% to 11.8% residual survival) at and between the gemcitabine-equivalent concentrations of 10^{-10} M and 10^{-8} M respectively (Figure 10). Similarly, gemcitabine alone created progressive and then rapid increases in cytotoxic anti-neoplatic potency from 5.6% to 88.3% (94.4% and 11.7% residual survival) at and between the gemcitabine-equivalent concentrations of 10^{-10} M and 10^{-7} M respectively (Figure 10). Gemcitabine in dual combination with mebendazole (0.15 μM fixed-concentration) was substantially more potent than gemcitabine alone at the gemcitabine-equivalent concentrations of 10^{-10} M (30.3% -versus- 5.6%), 10^{-9} M (28.3% -versus- 5.8%), 10^{-8} M (88.2% -versus- 24.3%) respectively (Figure 10). Mean maximum cytotoxic anti-neoplactic potencies for gemcitabine in dual combination with mebendazole (0.15 μM fixed-concentration) compared to gemcitabine alone were nearly identical at 90.1% versus 88.32 (9.9% and 11.7% residual survival) and 88.7% versus 92.5% (11.3% and 7.5% residual survival) at the gemcitabine-equivalent concentrations of 10^{-7} M and 10^{-6} M respectively (Figure 10).

Discussion

General

The molecular design and implementation of succinimidyl 4,4-azipentanoate in organic chemistry reactions schemes to create the UV-photoactivated gemcitabine-(C_4-*amide*) intermediate for the synthesis of gemcitabine-(C_4-*amide*)-[anti-HER2/*neu*] [40] or other covalent gemcitabine immunochemotherapeutics has not been extensively delineated to date. Somewhat analogous organic chemistry reaction schemes for the synthetic production of a covalent gemcitabine-(C_5-*methylhydroxy*)-[anti-HER2/*neu*] immunochemotherapeutic have been described in a limited number of investigations [20]. Gemcitabine-(C_4-*amide*)-[anti-HER2/*neu*] and the organic chemistry reactions utilized in the corresponding synthesis scheme offer several distinct advantages including gentler reaction conditions, greater retained biological activity (IgG binding avidity), greater end-product yield (due to less IgG degradation or polymerization), flexibility of prolonged storage of the UV-photoactivated chemotherapeutic intermediate, and implementation of a covalent bond forming moiety that lacks any aeromatic ring structure which is known to decrease the probability of inducting humor immune responses.

Cytotoxic anti-neoplastic potency

Increases in the molar chemotherapeutic-equivalent concentrations of gemcitabine-(C_4-*amide*)-[anti-HER2/*neu*] created declines in the survival of chemotherapeutic-resistant

mammary adenocarcinoma (SKBr-3) populations (Figures 4 and 9). Cytotoxic anti-neoplatic potency of gemcitabine-(C_4-*amide*)-[anti-HER2/*neu*] against chemotherapeutic-resistant mammary adenocarcinoma (SKBr-3) following an incubation period of 182-hours was very similar to gemcitabine alone after a shorter 72-hour incubation period (Figure 4). Gemcitabine-(C_4-*amide*)-[anti-HER2/*neu*] at the gemcitabine-equivalent concentrations of 10^{-7} M or 10^{-6} M during a 182-hour incubation period did not exert a substantially greater degree of selectively "targeted" anti-neoplastic potency against chemotherapeutic-resistant mammary adenocarcinoma (SKBr-3) compared to gemcitabine alone (Figures 4, 9 and 10). Such findings are in contrast to the measurably greater or equivalent levels of cytotoxic anti-neoplastic potency of covalent epirubicin-[anti-HER2/*neu*] immunochemotherapeutics compared to epirubicin alone [41-44]. Despite this diference, results imply that greater levels of selectively "*targeted*" cytotoxic anti-neoplastic potency could have been attained with gemcitabine-(C_4-*amide*)-[anti-HER2/*neu*] at incubation periods of duration greater than 182-hours (Figure 4).

Conceptually there are at least five analytical variables that could have alternatively been modified to achieve substantially higher total levels of cytotoxic anti-neoplastic potency for gemcitabine-(C_4-*amide*)-[anti-HER2/*neu*]. *First*, incubation times with chemotherapeutic-resistant mammary adenocarcinoma (SKBr-3) could have been lengthened to a period >182-hours [19] thereby allowing greater opportunity for larger amounts of gemcitabine to be internalized by receptor-mediated endocytosis and subsequently liberated intracellularly from gemcitabine-(C_4-*amide*)-[anti-HER2/*neu*]. Support for this consideration in based on the observation that there was a simple dose effect for gemcitabine-(C_4-*amide*)-[anti-HER2/*neu*], and because mammary adenocarcinoma (SKBr-3) survivability was very similar when challenged with either gemcibatine-(C_5-*methylcarbamate*)-[anti-HER2/*neu*] [20] or gemcitabine-(C4-amide)-[anti-HER2/neu] (182 hours) compared to gemcitabine (72-hours), which then increased dramatically for gemcitabine over an extended incubation period (182 hours) (Figures 4, 9 and 10) [20].

Second, cytotoxic anti-neoplastic potency of gemcibatine-(C_4-*amide*)-[anti-HER2/*neu*] could alternatively have been assessed against a non-chemotherapeutic-resistant human neoplastic cell type similar to those utilized to evaluate majority of the covalent biochemotherapeutics reported in the literature to date. Similarly, the cytotoxic anti-neoplatic potency of gemcibatine-(C_4-*amide*)-[anti-HER2/*neu*] could also have alternatively been measured against an entirely diferent neoplastic cell type such as pancreatic carcinoma [52] small-cell lung carcinoma [53] neuroblastoma, [54] or leukemia/lymphoid [55,56] due to their relatively higher gemcitabine sensitivity. In addition, human promyelocytic leukemia [24,55], T-4 lymphoblastoid clones [55], glioblastoma [24,55], cervical epitheliod carcinoma [55], colon adenocarcinoma [55], pancreatic adenocarcinoma [55], pulmonary adenocarcinoma [55], oral squamous cell carcinoma [55], and prostatic carcinoma [57] have been found to be sensitive to gemcitabine and covalent gemcitabine-(oxyether phopholipid) preparations. Within this array of neoplastic cell types both human mammary carcinoma (MCF-7/WT-2′) [55] and mammary adenocarcinoma (BG-1) [55] are known to be relatively more resistant to gemcitabine and gemcitabine-(oxyether phopholipid) chemotherapeutic conjugate. Presumably this pattern of gemcitabine sensitivity is directly relevant to the

cytotoxic anti-neoplatic potency detected for gemcibatine-(C_4-*amide*)-[anti-HER2/*neu*] in chemotherapeutic-resistant mammary adenocarcinoma (SKBr-3) populations (Figure 4).

Third, [^{3}H]-thymidine, or an ATP-based assay could have alternatively been applied to measure anti-neoplastic potency of gemcitabine-(C_4-*amide*)-[anti-HER2/*neu*] since they are reportedly >10-fold more sensitive in detecting early sub-lethal cell injury compared to MTT vitality stain assay methods [58,59]. Despite this consideration, MTT vitality stain continues to be extensively applied for the routine assessment of true cytotoxic anti-neoplastic potency in contrast to transient or sub-lethal injury for chemotherapeutics covalently incorporated synthetically into molecular platforms that provide properties of selective “targeted” delivery [24,44,55,60-66] In this context, one distinctly important attribute of MTT vitality stain based assays is that they provide a way of measuring the extent of cell death induced by an anti-cancer agent within a population of neoplastic cells in a manner that tends to have greater relevance to clinical oncology in contrast to assays for biomarkers that simply reflect transient (non-lethal) cell injury.

Fourth, cytotoxic anti-neoplastic potency of gemcibatine-(C_4-*amide*)-[anti-HER2/*neu*] immunochemotherapeutic could have been delineated *in-vivo* against human neoplastic xenographs in animal hosts as a model for human cancer. Many if not most covalent immunochemotherapeutics with properties of selective “targeted” delivery frequently have a higher degree of effectiveness and potency when evaluated *in-vivo* in contrast to levels acquired *ex-vivo* in tissue culture models utilizing the same cancer cell type [67-69]. Enhanced efficacy and potency is in part attributable to endogenous immune responses including antibody-dependent cell cytotoxicity (ADCC) phenomenon [70] in concert with complemented-mediated cytolysis induced by formation of antigen-immunoglobulin complexes on the exterior surface membrane of “targeted” neoplastic cell populations. During ADCC events cytotoxic components are liberated that additively and synergistically enhance the cytotoxic anti-neoplastic activity of conventional chemotherapeutic agents [71]. Contributions of ADCC and complement-mediated cytolysis to the *in-vivo* cytotoxic anti-neoplastic potency of covalent immunochemotherapeutics is further complemented by the additive and synergistic anti-neoplastic properties attained wiith anti-trophic receptor monoclonal immunoglobulin when applied in dual combination with conventional chemotherapeutic agents [72-83]. Additive or synergistic interactions of this type have been delineated between anti-HER2/*neu* when applied simultaneously with cyclophosphamide [79,81], docetaxel [79], doxorubicin [79,81], etoposide [79], methotrexate [79], paclitaxel [79,81] or vinblastine [79].

Fifth, strategies for the synthesis of gemcitabine-(C_4-*amide*)-[anti-HER2/neu] could have been modified to increase the gemcitabine molar-incorporation-index. Unfortunately, such modifiocations usually require the implementation of harsher reaction conditions that in turn impose a higher risk of reduced biological activity (e.g. IgG antigen binding avidity) and substantial declines in final/total product yield [69,84]. Aside from overly harsh synthesis conditions, excessively high molar incorporation indexes for any chemotherapeutic agent can also reduce biological integrity of immunoglobulin fractions when the number of pharmaceutical groups introduced into the Fab' antigen-binding region becomes excessive. Such alterations can result in only modest declines in immunoreactivity (e.g. 86% for a 73:1

ratio) but disproportionately large declines in anti-neoplastic activity in addition to reductions in potency that can decrease to levels substantially lower compared to the corresponding non-conjugated “free” chemotherapeutic (e.g. anthracyclines) [69].

Biological integrity of the immunoglobulin component of covalent immunochemotherapeutics is critically important because it facilitates selective “targeted” delivery of the chemotherapeutic moiety and it's subsequent internalization by mechanisms of receptor-mediated endocytosis when an appropriate site on the external membrane has been selected [85]. Immunoglobulin-induced receptor-mediated endocytosis at membrane HER2/*neu* complexes ultimately can result in increases in the intracellular concentration of selectively “targeted”/delivered chemotherapeutic that are 8.5 [86] to >100 × fold greater [87] than those attainable by simple passive diffusion. Although specific data for HER2/*neu a*nd EGFR expression by mammary adenocarcinoma (SKBr-3) is limited, [44] other neoplastic cell types like metastatic multiple myeloma are known to internalize approximately 8×10^6 molecules of anti-CD74 monoclonal antibody per day [88].

Cytotoxic anti-neoplastic potency of tubulin/microtubule inhibitors

Benzimadazole literature review—The benzimidazole class of anthelmintics within neoplastic cells exert a mechanism-of-action that is distinctly different, but still similar to that of the vinca alkaloids [89] which involves binding to colchicine-sensitive sites on β-tubulin protein. The ultimate effect is an inhibition of tubulin polymerization or induced tubulin de-polymerization with subsequent suppression of normal microtubule assembly and function necessary for successful completion of mitosis (cell cycle M-phase). Coincident with a disruption of mitosis, benzimidazole tubulin/microtubule inhibitors are believed to induce apoptosis in neoplastic cells through a variety of pathways based upon detection of elevations in Bcl-2 phosphorylation [90], capsase-3, [91-94] caspase-8 [94], caspase-9 [92,94], cytochrome-C release [91,92,94,95], p53 [92]. DNA laddering profiles [93] and DNA fragmentation (TUNEL) [93,94]. Declines in neoplastic cell growth and vitality induced by benzimidazole tubulin/microtubule inhibitors have been detected as a function of alterations in parameters that reflect G_2/M [93,94,96] and G_0-G_1 [96] arrest, decreased [^{3}H]thymidine incorporation [96] spheroid cell formation [92], altered cell vitality staining intensity [94], and suppression of growth kinetics [93]. Benzimidazoles also inhibit vascular endothelial growth factor receptor function (VEGFR) [97], and reduce expression of CD31 (tumor angiogenesis biomarker) [92,95], carcinoembryonic antigen (CEA: *in-vivo*) [98]; and α-feto protein (AFP: *in-vivo*) [98].

Te ultimate effect of benzimidazoles on cancer cell biology includes their ability to promote suppress migration/invasion (*in-vitro*) [92], metastasis (*in-vivo*) [92,95], and tumor growth rate (*in-vivo*) [95]. Preliminary experimental investigations have detected vulnerability of adrenocortical carcinoma (xenographs) [92], colorectal cancer [93,98], hepatocellular carcinoma [96,98], leukemia [89,91], lung cancer [95], (non-small cell [94,95]), melanoma (chemo-resistant) [90], myeloma [89], and ovarian cancer [96,97,99,100] to benzimidazole tubulin/microtubule inhibitors. The cytotoxic anti-neoplastic potency of the benzimidazole class of tubulin/microtubule inhibitors against breast cancer has previously remained largely unknown. In contrast to a single report for flubendazole, the creation of mammalian

chromosomal aberrations has to date not been described for either albendazole [93,97] or mebendazole [101].

Benzimadazole laboratory results—In chemotherapeutic-resistant mammary adenocarcinoma (SKBr-3) the benzimidazole tubulin/microtubule inhibitors albendazole, mebendazole and flubendazole each demonstrated detectable cytotoxic anti-neoplastic potency between a final concentration range of 0 μM to 2.5 μM that was similar to levels observed against other neoplastic cell types (Figures 6-8) [89-94]. Cytotoxic anti-neoplastic potencies for albendazole, flubendazole and mebendazole increased when the direct-contact incubation period was extended from 72-hours to 182 hours (Figures 6, 7 and 8). Flubendazole was the most potent benzimidazole while albendazole was substantially less potent than either flubendazole or mebendazole against chemotherapeutic-resistant mammary adenocarcinoma (SKBr-3) at benzimidazole-equivalent concentrations below 0.75 mM (Figures 6 and 7). The relative order of benzimidazole cytotoxic anti-neoplastic potency against chemotherapeutic-resistant mammary adenocarcinoma (SKBr-3) closely correlates with profiles recognized with other neoplastic cell types including leukemia [89] and myeloma [89] cell types at longer incubation periods (Figures 6 and 7) [40,41].

Dual combination cytotoxic anti-neoplastic potencies—The mechanism-of-action for the benzimidazoles is similar to the vinca alkaloids, taxanes (e.g. paclitaxel), podophyllotoxins (e.g. etoposide) and monomethyl auristatin E (MMAE). Based on these properties speculation suggests that benzimidazoles can additively or synergistically enhance the cytotoxic anti-neoplastic potency of conventional and selectively “targeted” chemotherapeutics. Such properties to date have largely remained unknown except for limited preliminary descriptions for dual vinblastine/benzimidazole combinations [89].

Significantly greater levels of cytotoxic anti-neoplastic potency were attained with gemcitabine-(C_4-*amide*)-[anti-HER2/*neu*] immunochemotherapeutic or gemcitabine alone when applied in dual combination with the mebendazole (Figures 9 and 10). Covalent gemcitabine-(C_4-*amide*)-[anti-HER2/*neu*] immunochemotherapetuic in dual combination with mebendazole (0.15 μM fixed-concentration) exerted significantly greater levels of cytotoxic anti-neoplastic potency than gemcitabine-(C_4-*amide*)-[anti-HER2/*neu*] alone between the gemcitabine-equivalent concentrations of 10^{-10} and 10^{-6} M (Figure 9). Maximum cytotoxic anti-neoplastic potency of gemcitabine-(C_4-*amide*)-[anti-HER2/*neu*] in combination with mebendazole (0.15 μM fixed-concentration) 68.8% (31.2% residual survival) was detected at the gemcitabine-equivalent concentration of 10^{-6} M (Figure 9). Gemcitabine in combination with mebendazole (0.15 μM fixed-concentration) was more potent than gemcitabine-(C_4-*amide*)-[anti-HER2/*neu*] in combination with mebendazole (0.15 μM fixed-concentration) and this trend was most prominent at the gemcitabine-equivalent concentrations of 10^{-8} M, 10^{-7} M, and 10^{-6} M (Figure 10). Gemcitabine chemotherapeutic alone compared to gemcitabine-(C_4-*amide*)-[anti-HER2/*neu*] in combination with mebendazole (0.15 μM fixed-concentration) both exerted somewhat similar profiles for cytotoxic anti-neoplastic potency within the lower gemcitabine-equivalent concentrations at and between 10^{-9} M and 10^{-8} M (Figure 10). Gemcitabine alone

tended to be more potent at the higher gemcitabine-equivalent concentrations of 10^{-7} M (88.3% -versus- 50.8%) and 10^{-6} M (92.5% -versus- 68.8%) respectively (Figure 10).

Te cytotoxic anti-neoplastic potency profiles for membendazole when applied in dual combination with a covalent gemcitabine-(C_4-*amide*)-[anti-HER2/*neu*] or gemcitabine illustrates the potential of the benzimidazoles to complement the efficacy of gemcitabine and covalent gemcitaibine immunochemotherapeutics (Figures 9 and 10). In direct correlation with these findings, benzimidazoles also (additively or synergistically) complement the cytotoxic anti-neo-plastic potency of epirubicin and covalent epirubicin immunoche-motherapeutics against chemotherapeutic-resistant mammary adenocarcinoma (SKBr-3) [41]. Undoubtedly, levels of cytotoxic anti-neoplastic potency for gemcitabine-(C_4-*amide*)-[anti-HER2/*neu*] immunochemotherapetuic in dual combination with mebendazole (0.15 μM fixed-concentration) would probably be measurably greater with the implementation of direct-contact incubation periods longer than 182-hours.

Conclusion

Organic chemistry reaction schemes have been developed to facilitate synthesis of gemcitabine-(C_4-*amide*)-[anti-HER2/*neu*] that possesses properties of selective “targeted” delivery that can also serve as a prototype or reference template for the molecular design and organic chemistry synthesis of similar covalent immunochemotherapeutic or ligand-chemotherapeutics. Attributes of the synthesis method include; [*i*] greater flexibility for conveniently covalently bonding gemcitabine and other chemotherapeutics with analogous chemical properties and molecular structure to large molecular weight platforms at a relatively high chemotherapeutic molar incorporation index; [*ii*] affords a lower risk of spontaneous immunoglobulin polymerization compared to synthesis methods dependent on protein pre-thiolation; [*iii*] utilization of synthesis conditions during covalent bond formation that impose a lower risk of promoting degradative fragmentation or large molecular weight polymerization; [*iv*] design and synthesis of covalent chemotherapeutic-ligands or immunochemotherapeutics that can employ a spectrum of large molecular weight platforms that possess an array of different selective “targeted” delivery properties; and an [*v*] option to generate a reactive chemotherapeutic intermediate that can be stored for prolonged periods for future application.

Cytotoxic anti-neoplastic potencies for gemcitabine-(C_4-*amide*)-[anti-HER2/*neu*] at the end of a 182-hour incubation period were similar to gemcitabine following a 72-hour incubation period in populations of chemotherapeutic-resistant mammary adenocarcinoma (SKBr-3). Cytotoxic anti-neoplastic potency of gemcitabine-(C_4-*amide*)-[anti-HER2/*neu*] would likely have been greater if it had been evaluated using an incubation period greater than 182-hours or had been determined against human promyelocytic leukemia, T-4 lymphoblastoid clones, glioblastoma; cervical epitheliod carcinoma, colon adenocarcinoma, pancreatic adenocarcinoma, pulmonary adenocarcinoma, oral squamous cell carcinoma, or prostatic carcinoma. Parallel investigations delineated the relative cytotoxic anti-neoplastic potency of the benzimidazole tubulin/microtubule inhibitors, albendazole, flubendazole, and mebendazole against chemotherapeutic-resistant mammary adenocarcinoma (SKBr-3). Mebendazole in dual combination with gemcitabine or gemcitabine-(C_4-*amide*)-[anti-HER2/

neu] resulted in levels of cytotoxic anti-neoplastic potency that were greater than those obtained with either gemcitabine or gemcitabine-(C_4-*amide*)-[anti-HER2/*neu*] respectively.

Discovery and preliminary characterization of the cytotoxic anti-neoplastic properties of gemcitabine-(C_4-*amide*)-[anti-HER2/*neu*] and benzimidazoles in addition to the enhanced levels of efficacy achieved with dual combinations against chemotherapeutic-resistant mammary adenocarcinoma (SKBr-3) has several important implications. Such dual combinations offers the potential option for developing treatment schemes that more rapidly evoke durable (long-term) resolution of neoplastic disease states that are at least in part attainable because both the benzimidazoles [102-104] and chemotherapeutics covalently bound to large molecular weight platforms are apparently poor substrates for P-glycoprotein/MDR-1 (multi-drug resistance efflux pump) [24,105]. Accompanying their potential to effectively resolve neoplastic conditions, covalent gemcitabine immunochemotherapeutics, gemcitabine or other conventional chemotherapeutic agents in dual additive or synergistic combination with benzimidazoles represent a therapeutic regimen option for implementation in clinical oncology that may have a relatively wide safety index due to of fewer and less severe sequelae. Conceptually, such attributes collectively can at least theoretically be attained because of the relatively wide safety index for both the benzimidazoles compared to many if not most conventional chemotherapeutics [93,98,99,106] in addition to the selective "targeted" delivery properties of covalent immunochemotherapeutics. Collectively each of these attributes can contribute to realizing enhanced levels of cytotoxic anti-neoplastic potency which can ultimately facilitate both a more rapid resolution of neoplastic conditions and a lowering of total chemotherapeutic dosage requirements can further reduce the frequency and severity of sequelae plus decrease the probabilty of resistance developing during prolonged administration protocols. Lastly, from a clinical oncology perspective, the application of either a covalent gemcitabine immunochemotherapeutic or gemcitabine in dual combination with benzimidazole tubulin/microtubule inhibitors directly coincides with the general recommendation for *in-vivo* treatment regimens. Such guidelines in part advocate administration of diferent anti-cancer agent classes during the course of multi-chemotherapeutic regimens that ideally exert different mechanisms-of-action (avoids competitive inhibition) and individually precipitate distinctly different sets of undesirable sequellae.

Acknowledgments

The authors would like to acknowledge Mr. Tom Thompson in the Office of Agriculture Communications for assistance with the photographic illustration.

References

1. Gong C, Yao Y, Wang Y, Liu B, Wu W, et al. Up-regulation of miR-21 mediates resistance to trastuzumab therapy for breast cancer. J Biol Chem. 2011; 286:19127–19137. [PubMed: 21471222]
2. Lewis Phillips GD, Li G, Dugger DL, Crocker LM, Parsons KL, et al. Targeting HER2-positive breast cancer with trastuzumab-DM1, an antibody-cytotoxic drug conjugate. Cancer Res. 2008; 68:9280–9290. [PubMed: 19010901]
3. Pandya K, Meeke K, Clementz A, Rogowski A, Roberts J, et al. Targeting both Notch and ErbB-2 signalling pathways is required for prevention of ErbB-2-positive breast tumour recurrence. Br J Cancer. 2011; 105:796–806. [PubMed: 21847123]

4. Scaltriti M, Eichhorn PJ, Cortés J, Prudkin L, Aura C, et al. Cyclin E amplification/overexpression is a mechanism of trastuzumab resistance in HER2+ breast cancer patients. Proc Natl Acad Sci. 2011; 108:3761–3766. [PubMed: 21321214]
5. Sliwkowski MX, Lofgren JA, Lewis GD, Hotaling TE, Fendly BM, et al. Nonclinical studies addressing the mechanism of action of trastuzumab (Herceptin). Semin Oncol. 1999; 26:60–70. [PubMed: 10482195]
6. Morgillo F, Woo JK, Kim ES, Hong WK, Lee HY. Heterodimerization of insulin-like growth factor receptor/epidermal growth factor receptor and induction of surviving expression counteract the anti-tumor action of Erlotinib. Cancer Res. 2006; 66:10100–10111. [PubMed: 17047074]
7. Morgillo F, Kim W, Kim E, Ciardiello F, Hong W, et al. Implications of the insulin-like growth factor-IR pathway in the resistance of non-small cell lung cancer cells to treatment with geftinib. Clin Cancer Res. 2007; 13:2795–2803. [PubMed: 17473213]
8. Sartore-Bianchi A, Di Nicolantonio F, Nichelatti M, Molinari F, De Dosso S, et al. Multi-determinants analysis of molecular alterations for predicting clinical benefit to EGFR-targeted monoclonal antibodies in colorectal cancer. PLoS ONE. 2009; 4:e7287. [PubMed: 19806185]
9. Weickhardt AJ, Tebbutt NC, Mariadason JM. Strategies for overcoming inherent and acquired resistance to EGFR inhibitors by targeting downstream effectors in the RAS/PI3K pathway. Curr Cancer Drug Targets. 2010; 10:824–833. [PubMed: 20718704]
10. Dempke WC, Heinemann V. Ras mutational status is a biomarker for resistance to EGFR inhibitors in colorectal carcinoma. Anticancer Res. 2010; 30:4673–4677. [PubMed: 21115922]
11. Modjtahedi H, Essapen S. Epidermal growth factor receptor inhibitors in cancer treatment: advances, challenges and opportunities. Anticancer Drugs. 2009; 20:851–855. [PubMed: 19826350]
12. Barok M, Tanner M, Köninki K, Isola J. Trastuzumab-DM1 causes tumour growth inhibition by mitotic catastrophe in trastuzumab-resistant breast cancer cells in-vivo. Breast Cancer Res. 2011; 13:R46. [PubMed: 21510863]
13. Köninki K, Barok M, Tanner M, Staff S, Pitkänen J, et al. Multiple molecular mechanisms underlying trastuzumab and lapatinib resistance in JIMT-1 breast cancer cells. Cancer Lett. 2010; 294:211–219. [PubMed: 20193978]
14. Mitra D, Brumlik MJ, Okamgba SU, Zhu Y, Duplessis TT, et al. An oncogenic isoform of HER2 associated with locally disseminated breast cancer and trastuzumab resistance. Mol Cancer Ther. 2009; 8:2152–2162. [PubMed: 19671734]
15. Oliveras-Ferraros C, Vazquez-Martin A, Cufí S, Torres-Garcia VZ, Sauri-Nadal T, et al. Inhibitor of Apoptosis (IAP) survivin is indispensable for survival of HER2 gene-amplified breast cancer cells with primary resistance to HER1/2-targeted therapies. Biochem Biophys Res Commun. 2011; 407:412–419. [PubMed: 21402055]
16. Oliveras-Ferraros C, Vazquez-Martin A, Martin-Castilló B, Pérez-Martínez MC, Cufí S, et al. Pathway-focused proteomic signatures in HER2-overexpressing breast cancer with a basal-like phenotype: new insights into de novo resistance to trastuzumab (Herceptin). Int J Oncol. 2010; 37:669–678. [PubMed: 20664936]
17. Ritter CA, Perez-Torres M, Rinehart C, Guix M, Dugger T, et al. Human breast cancer cells selected for resistance to trastuzumab in-vivo overexpress epidermal growth factor receptor and ErbB ligands and remain dependent on the ErbB receptor network. Clin Cancer Res. 2007; 13:4909–4919. [PubMed: 17699871]
18. Ali SM, Khan AR, Ahmad MU, Chen P, Sheikh S, et al. Synthesis and biological evaluation of gemcitabine-lipid conjugate (NEO6002). Bioorg Med Chem Lett. 2005; 15:2571–2574. [PubMed: 15863318]
19. Lansakara-P DS, Rodriguez BL, Cui Z. Synthesis and in-vitro evaluation of novel lipophilic monophosphorylated gemcitabine derivatives and their nanoparticles. Int J Pharm. 2012; 429:123–134. [PubMed: 22425885]
20. Coyne CP, Jones T, Pharr T. Synthesis of a covalent gemcitabine-(carbamate)-[anti-HER2/neu] immunochemotherapeutic and cytotoxic anti-neoplastic activity against chemotherapeutic-resistant SKBr-3 mammary carcinoma. Bioorg Med Chem. 2011; 19:67–76. [PubMed: 21169024]

21. Gilbert JA, Salavaggione OE, Ji Y, Pelleymounter LL, Eckloff BW, et al. Gemcitabine pharmacogenomics: cytidine deaminase and deoxycytidylate deaminase gene resequencing and functional genomics. Clin Cancer Res. 2006; 12:1794–1803. [PubMed: 16551864]
22. Giovannetti E, Laan AC, Vasile E, Tibaldi C, Nannizzi S, et al. Correlation between cytidine deaminase genotype and gemcitabine deamination in blood samples. Nucleosides Nucleotides Nucleic Acids. 2008; 27:720–725. [PubMed: 18600531]
23. Shamseddine AI, Khalifeh MJ, Mourad FH, Chehal AA, Al-Kutoubi A, et al. Comparative pharmacokinetics and metabolic pathway of gemcitabine during intravenous and intra-arterial delivery in unresectable pancreatic cancer patients. Clin Pharmacokinet. 2005; 44:957–967. [PubMed: 16122282]
24. Alexander RL, Greene BT, Torti SV, Kucera GL. A novel phospholipid gemcitabine conjugate is able to bypass three drug-resistance mechanisms. Cancer Chemother Pharmacol. 2005; 56:15–21. [PubMed: 15789226]
25. Colomer R, Llombart-Cussac A, Tusquets I, Rifà J, Mayordomo JI, et al. Biweekly gemcitabine plus vinorelbine in first-line metastatic breastcancer: efficacy and correlation with HER2 extracellular domain. Clin Transl Oncol. 2006; 8:896–902. [PubMed: 17169763]
26. Hortobagyi GN. Treatment of advanced breast cancer with gemcitabine and vinorelbine. Oncology (Williston Park). 2001; 15:15–17. [PubMed: 11252883]
27. Martín M, Ruiz A, Muñoz M, Balil A, García-Mata J, et al. Gemcitabine plus vinorelbine versus vinorelbine monotherapy in patients with metastatic breast cancer previously treated with anthracyclines and taxanes: final results of the phase III Spanish Breast Cancer Research Group (GEICAM) trial. Lancet Oncol. 2007; 8:219–225. [PubMed: 17329192]
28. Qu G, Perez EA. Gemcitabine and targeted therapy in metastatic breast cancer. Semin Oncol. 2002; 29:44–52. [PubMed: 12138397]
29. Colomer R. Gemcitabine in combination with paclitaxel for the treatment of metastatic breast cancer. Womens Health (Lond Engl). 2005; 1:323–329. [PubMed: 19803874]
30. Colomer R. What is the best schedule for administration of gemcitabine-taxane? Cancer Treat Rev. 2005; 31:S23–S28. [PubMed: 16360544]
31. Biesma B, Smit EF, Postmus PE. A dose and schedule finding study of gemcitabine and etoposide in patients with progressive non-small cell lung cancer after platinum containing chemotherapy. Lung Cancer. 1999; 24:115–121. [PubMed: 10444062]
32. Hansen HH, Rørth M. Lung Cancer. Cancer Chemother Biol Response Modif. 1997; 17:444–463. [PubMed: 9551225]
33. Melnik MK, Webb CP, Richardson PJ, Luttenton CR, Campbell AD, et al. Phase II Trial to Evaluate Gemcitabine and Etoposide for Locally Advanced or Metastatic Pancreatic Cancer. Mol Cancer Ther. 2010; 9:2423–2429. [PubMed: 20682649]
34. Ofazoglu E, Kissler KM, Sievers EL, Grewal IS, Gerber HP. Combination of the anti-CD30-auristatin-E antibody-drug conjugate (SGN-35) with chemotherapy improves antitumour activity in Hodgkin lymphoma. Br J Haematol. 2008; 142:69–73. [PubMed: 18477046]
35. Kirstein MN, Hassan I, Guire DE, Weller DR, Dagit JW, et al. High-performance liquid chromatographic method for the determination of gemcitabine and 2′,2′-difuorodeoxyuridine in plasma and tissue culture media. J Chromatogr B Analyt Technol Biomed Life Sci. 2006; 835:136–142.
36. Reichelova V, Albertioni F, Liliemark J. Determination of 2-chloro-2′-deoxyadenosine nucleotides in leukemic cells by ion-pair high-performance liquid chromatography. J Chromatogr B Biomed Appl. 1996; 682:115–123. [PubMed: 8832432]
37. Reichelova V, Albertioni F, Liliemark J. Determination of 2-chloro-2′-deoxyadenosine nucleotides in leukemic cells by ion-pair high-performance liquid chromatography. J Chromatogr B Biomed Appl. 1996; 682:115–123. [PubMed: 8832432]
38. Hempel G, Schulze-Westhoff P, Flege S, Laubrock N, Boos J. Therapeutic drug monitoring of doxorubicin in paediatric oncology using capillary electrophoresis. Electrophoresis. 1998; 19:2939–2943. [PubMed: 9870393]

39. Ulbrich K, Etrych T, Chytil P, Jelinkova M, Rihova B. HPMA copolymers with pH-controlled release of doxorubicin: In-vitro cytotoxicity and in-vivo antitumor activity. J Control Release. 2003; 87:33–47. [PubMed: 12618021]
40. Coyne CP, Jones T, Bear R. Synthesis of gemcitabine-(C4-amide)-[anti-HER2/neu] utilizing a UV-photoactivated gemcitabine intermediate: cytotoxic anti-Neoplastic activity against chemotherapeutic-resistant mammary adenocarcinoma SKBr-3. Journal of Cancer Therapy. Breast Cancer Special Issue. 2012; 3:689–711.
41. Coyne CP, Jones T, Bear R. Influence of alternative tubulin inhibitors on the potency of epirubicin-SS-anti-HER2/neu synthesized with a UV-activated intermediate. Cancer and Clinical Oncology. 2012; 1:49–80. [PubMed: 26225190]
42. Coyne CP, Jones T, Bear R. Synthesis of a Covalent Epirubicin-(C3-amide)-Anti-HER2/neu Immunochemotherapeutic Utilizing a UV-Photoactivated Anthracycline Intermediate. Cancer Biotherapy and Radiopharmaceuticals. 2012; 27:41–55. [PubMed: 22191802]
43. Coyne CP, Jones T, Sygula A, Bailey J, Pinchuk L. Epirubicin-[anti-HER2/neu] synthesized with an epirubicin-(C13-imino)-EMCS analog: Anti-neoplastic activity against chemotherapeutic-resistant SKBr-3 mammary carcinoma in combination with organic selenium. Journal of Cancer Therapy. 2011; 2:22–39. [PubMed: 26229727]
44. Coyne CP, Ross MK, Bailey JG. Dual potency anti-HER2/neu and anti-EGFR anthracycline-immunoconjugates in chemotherapeutic-resistant mammary carcinoma combined with cyclosporin-A and verapamil P-glycoprotein inhibition. J Drug Targeting. 2009; 17:474–489.
45. Beyer U, Rothen-Rutishauser B, Unger C, Wunderli-Allenspach H, Kratz F. Difference in the intracellular distribution of acid-sensitive doxorubicin-protein conjugates in comparison to free and liposomal-formulated doxorubicin as shown by confocal microscopy. Pharm Res. 2001; 18:29–38. [PubMed: 11336350]
46. Di Stefano G, Lanza M, Kratz F, Merina L, Fiume L. A novel method for coupling doxorubicin to lactosaminated human albumin by an acid sensitive hydrazone bond: synthesis, characterization and preliminary biological properties of the conjugate. Eur J Pharm Sci. 2004; 23:393–397. [PubMed: 15567293]
47. Sinkule JA, Rosen ST, Radosevich JA. Monoclonal antibody 44-3A6 doxorubicin immunoconjugates: comparative in vitro anti-tumor efficacy of different conjugation methods. Tumour Biol. 1991; 12:198–206. [PubMed: 1651554]
48. Dillman RO, Johnson DE, Ogden J, Beidler D. Significance of antigen, drug, and tumor cell targets in the preclinical evaluation of doxorubicin, daunorubicin, methotrexate, and mitomycin-C monoclonal antibody immunoconjugates. Mol Biother. 1989; 1:250–255. [PubMed: 2515870]
49. Sapra P, Stein R, Pickett J, Qu Z, Govindan SV, et al. Anti-CD74 antibody-doxorubicin conjugate, IMMU-110, in a human multiple myeloma xenograph and in monkeys. Clin Cancer Res. 2005; 11:5257–5264. [PubMed: 16033844]
50. Sivam GP, Martin PJ, Reisfeld RA, Mueller BM. Therapeutic efficacy of a doxorubicin immunoconjugate in a preclinical model of spontaneous metastatic human melanoma. Cancer Res. 1995; 55:2352–2356. [PubMed: 7757986]
51. Yang HM, Reisfeld RA. Doxorubicin conjugated with monoclonal antibody directed to a human melanoma-associated proteoglycan suppresses growth of established tumor xenografts in nude mice. Proc Natl Acad Sci USA. 1988; 85:1189–1193. [PubMed: 3422487]
52. Michalski CW, Erkan M, Sauliunaite D, Giese T, Stratmann R, et al. Ex vivo chemosensitivity testing and gene expression profiling predict response towards adjuvant gemcitabine treatment in pancreatic cancer. Br J Cancer. 2008; 99:760–767. [PubMed: 18728667]
53. Hoang T, Kim K, Jaslowski A, Koch P, Beatty P, et al. Phase II study of second-line gemcitabine in sensitive or refractory small cell lung cancer. Lung Cancer. 2003; 42:7–102.
54. Bierau J, van Gennip AH, Leen R, Meinsma R, Caron HN, et al. Cyclopentenyl cytosine-induced activation of deoxycytidine kinase increases gemcitabine anabolism and cytotoxicity in neuroblastoma. Cancer Chemother Pharmacol. 2006; 57:105–113. [PubMed: 16133534]
55. Bierau J, van Gennip AH, Leen R, Meinsma R, Caron HN, van Kuilenburg AB. Cyclopentenyl cytosine-induced activation of deoxycytidine kinase increases gemcitabine anabolism and

cytotoxicity in neuroblastoma. Cancer Chemother Pharmacol. 2006; 57:105–113. [PubMed: 16133534]

56. Santini V, D'Ippolito G, Bernabei PA, Zoccolante A, Ermini A, et al. Effects of fludarabine and gemcitabine on human acute myeloid leukemia cell line HL 60: direct comparison of cytotoxicity and cellular Ara-C uptake enhancement. Leuk Res. 1996; 20:37–45. [PubMed: 8632676]
57. Lammers T, Subr V, Ulbrich K, Peschke P, Huber PE, et al. Simultaneous delivery of doxorubicin and gemcitabine to tumors in vivo using prototypic polymeric drug carriers. Biomaterials. 2009; 30:3466–3475. [PubMed: 19304320]
58. Mueller H, Kassack MU, Wiese M. Comparison of the usefulness of the MTT, ATP and calcein assays to predict the potency of cytotoxic agents in various human cancer cell lines. J Biomol Screen. 2004; 9:506–515. [PubMed: 15452337]
59. Ulukaya E, Ozdikicioglu F, Oral AY, Dermirci M. The MTT assay yields a relatively lower result of growth inhibition than the ATP assay depending on the chemotherapeutic drug tested. Toxicol In Vitro. 2008; 22:232–239. [PubMed: 17904330]
60. Denora N, Laquintana V, Trapani A, Lopedota A, Latrofa A, et al. Translocator protein (TSPO) ligand-Ara-C (cytarabine) conjugates as a strategy to deliver antineoplastic drugs and to enhance drug clinical potential. Mol Pharm. 2010; 7:2255–2269. [PubMed: 20958082]
61. Dery MC, Van Themsche C, Provencher D, Mes-Masson AM, Asselin E. Characterization of EN-1078D, a poorly differentiated human endometrial carcinoma cell line: a novel tool to study endometrial invasion in-vitro. Reprod Biol Endocrinol. 2007; 5:38–39. [PubMed: 17894888]
62. Huang H, Pierstorff E, Osawa E, Ho D. Active nanodiamond hydrogels for chemotherapeutic delivery. Nano Lett. 2007; 7:3305–3314. [PubMed: 17918903]
63. Kars MD, Iseri OD, Gunduz U, Molnar J. Reversal of multidrug resistance by synthetic and natural compounds in drug-resistant MCF-7 cell lines. Chemotherapy. 2008; 54:194–200. [PubMed: 18560226]
64. Kiew LV, Cheong SK, Sidik K, Chung LY. Improved plasma stability and sustained release profile of gemcitabine via polypeptide conjugation. Int J Pharm. 2010; 391:212–220. [PubMed: 20214970]
65. Spee B, Jonkers MD, Arends B, Rutteman GR, Rothuizen J, et al. Specific down-regulation of XIAP with RNA interference enhances the sensitivity of canine tumor cell-lines to TRAIL and doxorubicin. Mol Cancer. 2006; 5:34. [PubMed: 16953886]
66. Varache-Lembège M, Larrouture S, Montaudon D, Robert J, Nuhrich A. Synthesis and antiproliferative activity of aryl- and heteroaryl-hydrazones derived from xanthone carbaldehydes. Eur J Med Chem. 2008; 43:1336–1343. [PubMed: 17949859]
67. Aboud-Pirak E, Hurwitz E, Bellot F, Schlessinger J, Sela M. Inhibition of human tumor growth in nude mice by a conjugate of doxorubicin with monoclonal antibodies to epidermal growth factor receptor. Proc Natl Acad Sci USA. 1989; 86:3778–3781. [PubMed: 2786202]
68. Shen WC, Ryser HJ. cis-Aconityl spacer between daunomycin and macromolecular carriers: a model of pH-sensitive linkage releasing drug from a lysosomotrophic conjugates. Biochem Biophys Res Commun. 1981; 102:1048–1054. [PubMed: 7306187]
69. Zhang YT, Wang NQ, Li N, Liu T, Dong ZW. The antitumor effect of adriamycin conjugated with monoclonal antibody against gastric cancer in-vitro and in-vivo. Acta Pharmaceutica Sinica. 1992; 27:325–330. [PubMed: 1442051]
70. Barok M, Isola J, Pályi-Krekk Z, Nagy P, Juhász I, et al. Trastuzumab causes antibody-dependent cellular cytotoxicity-mediated growth inhibition of submacroscopic JIMT-1 breast cancer xenografts despite intrinsic drug resistance. Mol Cancer Ther. 2007; 6:2065–2072. [PubMed: 17620435]
71. Coyne CP, Fenwick BW, Ainsworth J. Cytotoxic activity of doxorubicin “loaded” neutrophils against human mammary carcinoma (HTB-19). Biotherapy. 1997; 10:145–159. [PubMed: 9373737]
72. Ciardiello F, Bianco R, Damiano V, De Lorenzo S, Pepe S, et al. Antitumor activity of sequential treatment with topotecan and anti-epidermal growth factor receptor monoclonal antibody C225. Clin Cancer Res. 1999; 5:909–916. [PubMed: 10213228]

73. Fry AK, Schilke KF, McGuire J, Bird KE. Synthesis and anticoagulant activity of heparin immobilized “end-on” to polystyrene microspheres coated with end-group activated polyethylene oxide. J Biomed Mater Res B Appl Biomater. 2010; 94:187–195. [PubMed: 20524194]
74. García-Sáenz JA, Martín M, Calles A, Bueno C, Rodríguez L, et al. Bevacizumab in combination with metronomic chemotherapy in patients with anthracycline- and taxane-refractory breast cancer. J Chemother. 2008; 20:632–639. [PubMed: 19028628]
75. Jin R, Moreira Teixeira LS, Krouwels A, Dijkstra PJ, van Blitterswijk CA, et al. Synthesis and characterization of hyaluronic acid-poly(ethylene glycol) hydrogels via Michael addition: An injectable biomaterial for cartilage repair. Acta Biomater. 2010; 6:1968–1977. [PubMed: 20025999]
76. Kim S, Prichard CN, Younes MN, Yazici YD, Jasser SA, et al. Cetuximab and irinotecan interact synergistically to inhibit the growth of orthotopic anaplastic thyroid carcinoma xenografts in nude mice. Clin Cancer Res. 2006; 12:600–607. [PubMed: 16428506]
77. Landriscina M, Maddalena F, Fabiano A, Piscazzi A, La Macchia O, et al. Erlotinib enhances the proapoptotic activity of cytotoxic agents and synergizes with paclitaxel in poorly-differentiated thyroid carcinoma cells. Anticancer Res. 2010; 30:473–480. [PubMed: 20332457]
78. Lynn KD, Udugamasooriya DG, Roland CL, Castrillon DH, Kodadek TJ, et al. GU81, a VEGFR2 antagonist peptoid, enhances the anti-tumor activity of doxorubicin in the murine MMTV-PyMT transgenic model of breast cancer. BMC Cancer. 2010; 10:397. [PubMed: 20673348]
79. Pegram MD, Lopez A, Konecny G, Slamon DJ. Trastuzumab and chemotherapeutics: drug interactions and synergies. Semin Oncol. 2000; 27:21–25. [PubMed: 11236023]
80. Slamon D, Pegram M. Rationale for trastuzumab (Herceptin) in adjuvant breast cancer trials. Semin Oncol. 2001; 28:13–19. [PubMed: 11301370]
81. Slamon DJ, Leyland-Jone B, Shak S, Fuchs H, Paton V, et al. Use of chemotherapy plus monoclonal antibody against HER2 for metastatic breast cancer that overexpress HER2. N Engl J Med. 2001; 344:786–792.
82. Winer EP, Burstein HJ. New combinations with Herceptin in metastatic breast cancer. Oncology. 2001; 61:50–57. [PubMed: 11694788]
83. Zhang L, Yu D, Hicklin DJ, Hannay JA, Ellis LM, et al. Combined anti-fetal liver kinase 1 monoclonal antibody (anti-VEGFR) and continuous low-dose doxorubicin inhibits angiogenesis and growth of human soft tissue sarcoma xenografts by induction of endothelial cell apoptosis. Cancer Res. 2002; 62:2034–2042. [PubMed: 11929822]
84. Greenfield RS, Kaneko T, Daues A, Edson MA, Fitzgerald KA, et al. Evaluation in-vitro of adriamycin immunoconjugates synthesized using an acid-sensitive hydrazone linker. Cancer Res. 1990; 50:6600–6607. [PubMed: 2208122]
85. Shih LB, Goldenberg DM, Xuan H, Lu HW, Mattes MJ, et al. Internalization of an intact doxorubicin immunoconjugate. Cancer Immunol Immunother. 1994; 38:92–98. [PubMed: 8306371]
86. Stan AC, Radu DL, Casares S, Bona CA, Brumeanu TD. Antineoplastic efficacy of doxorubicin enzymatically assembled on galactose residues of a monoclonal antibody specific for the carcinoembryonic antigen. Cancer Res. 1999; 59:115–121. [PubMed: 9892195]
87. Pimm MV, Paul MA, Ogumuyiwa T, Baldwin RW. Biodistribution and tumour localization of a daunomycin-monoclonal antibody conjugate in nude mice and human tumour xenografts. Cancer Immunol Immunother. 1988; 27:267–271. [PubMed: 3180150]
88. Hansen HJ, Ong GL, Diril H, Valdez A, Roche PA, et al. Internalization and catabolism of radiolabeled antibodies to the MHC class-II invariant chain by B-cell lymphomas. Biochem J. 1996; 320:293–300. [PubMed: 8947500]
89. Spagnuolo PA, Hu J, Hurren R, Wang X, Gronda M, et al. The antihelmintic flubendazole inhibits microtubule function through a mechanism distinct from Vinca alkaloids and displays preclinical activity in leukemia and myeloma. Blood. 2010; 115:4824–4833. [PubMed: 20348394]
90. Doudican N, Rodriguez A, Osman I, Orlow SJ. Mebendazole induces apoptosis via Bcl-2 inactivation in chemoresistant melanoma cells. Mol Cancer Res. 2008; 6:1308–1315. [PubMed: 18667591]

91. Khalilzadeh A, Wangoo KT, Morris DL, Pourgholami MH. Epothilone-paclitaxel resistant leukemic cells CEM/dEpoB300 are sensitive to albendazole: Involvement of apoptotic pathways. Biochem Pharmacol. 2007; 74:407–414. [PubMed: 17560963]

92. Martarelli D, Pompei P, Baldi C, Mazzoni G. Mebendazole inhibits growth of human adrenocortical carcinoma cell lines implanted in nude mice. Cancer Chemother Pharmacol. 2008; 61:809–817. [PubMed: 17581752]

93. Pourgholami MH, Akhter J, Wang L, Lu Y, Morris DL. Antitumor activity of albendazole against the human colorectal cancer cell line HT-29: in vitro and in a xenograft model of peritoneal carcinomatosis. Cancer Chemother Pharmacol. 2005; 55:425–432. [PubMed: 15565325]

94. Sasaki J, Ramesh R, Chada S, Gomyo Y, Roth JA, et al. The anthelmintic drug mebendazole induces mitotic arrest and apoptosis by depolymerizing tubulin in non-small cell lung cancer cells. Mol Cancer Ther. 2002; 1:1201–1209. [PubMed: 12479701]

95. Mukhopadhyay T, Sasaki J, Ramesh R, Roth JA. Mebendazole elicits a potent antitumor effect on human cancer cell lines both in-vitro and in-vivo. Clin Cancer Res. 2002; 8:2963–2969. [PubMed: 12231542]

96. Pourgholami MH, Woon L, Almajd R, Akhter J, Bowery P, et al. In-vitro and in-vivo suppression of growth of hepatocellular carcinoma cells by albendazole. Cancer Lett. 2001; 165:43–49. [PubMed: 11248417]

97. Pourgholami MH, Yan Cai Z, Lu Y, Wang L, Morris DL. Albendazole: a potent inhibitor of vascular endothelial growth factor and malignant ascites formation in OVCAR-3 tumor-bearing nude mice. Clin Cancer Res. 2011; 12:1928–1935. [PubMed: 16551879]

98. Morris DL, Jourdan JL, Pourgholami MH. Pilot study of albendazole in patients with advanced malignancy. Effect on serum tumor markers and high incidence of neutropenia. Oncology. 2001; 61:42–46. [PubMed: 11474247]

99. Pourgholami MH, Cai ZY, Badar S, Wangoo K, Poruchynsky MS, et al. Potent inhibition of tumoral hypoxia-inducible factor 1alpha by albendazole. BMC Cancer. 2010; 10:143. [PubMed: 20398289]

100. Pourgholami MH, Cai ZY, Wang L, Badar S, Links M, et al. Inhibition of cell proliferation, vascular endothelial growth factor and tumor growth by albendazole. Cancer Invest. 2009; 27:171–177. [PubMed: 19235589]

101. Nianjun H, Cerepnalkoski L, Nwankwo JO, Dews M, Landolph JR. Induction of chromosomal aberrations, cytotoxicity, and morphological transformation in mammalian cells by the antiparasitic drug flubendazole and the antineoplastic drug harringtonine. Fundam Appl Toxicol. 1994; 22:304–313. [PubMed: 8005380]

102. Dupuy J, Alvinerie M, Ménez C, Lespine A. Interaction of anthelmintic drugs with P-glycoprotein in recombinant LLC-PK1-mdr1a cells. Chem Biol Interact. 2010; 186:280–286. [PubMed: 20513441]

103. Merino G, Alvarez AI, Prieto JG, Kim RB. The anthelminthic agent albendazole does not interact with p-glycoprotein. Drug Metab Dispos. 2002; 30:365–369. [PubMed: 11901088]

104. Merino G, Jonker JW, Wagenaar E, Pulido MM, Molina AJ, et al. Transport of anthelmintic benzimidazole drugs by breast cancer resistance protein (BCRP/ABCG2). Drug Metab Dispos. 2005; 33:614–618. [PubMed: 15703302]

105. Bidwell GL, Davis AN, Fokt I, Priebe W, Raucher D. A thermally targeted elastin-like polypeptide-doxorubicin conjugate overcomes drug resistance. Invest New Drugs. 2007; 25:313–326. [PubMed: 17483874]

106. de Silva N, Guyatt H, Bundy D. Anthelmintics: a comparative review of their clinical pharmacology. Drugs. 1997; 53:769–788. [PubMed: 9129865]

Abbreviation

HER2/*neu*	trophic membrane receptor complex over-expressed by several neoplastic cell types

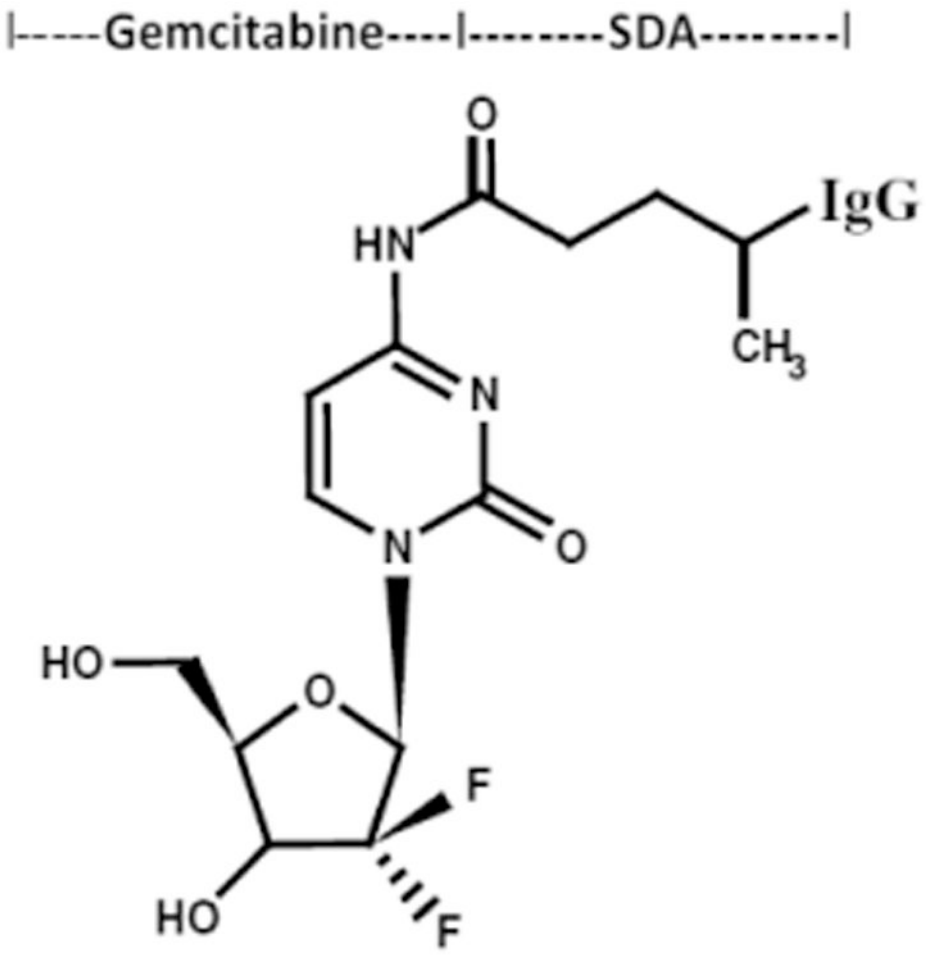

Figure 1.

Schematic illustration of the molecular design and chemical structure of the covalent immunochemotherapeutic, gemcitabine-(C_4-*amide*)-[anti-HER2/*neu*] synthesized utilizing a 2-stage organic chemistry reaction scheme that initially generates a gemcitabine UV-photoactivated intermediate.

Figure 2.

Characterization of the major molecular weight profile for covalent gemcitabine-(C_4-*amide*)-[anti-HER2/*neu*] immunochemotherapeutics compared to anti-HER2/*neu* monoclonal immunoglobulin. *Legends*: (*Lane-1)* murine anti-human HER2/*neu* monoclonal immunoglobulin reference control; and (*Lane-2*) covalent gemcitabine-(C_4-*amide*)-[anti-HER2/*neu*] immunochemotherapeutic. Covalent gemcitabine immunochemotherapeutic and anti-HER2/neu monoclonal immunoglobulin were size-separated by non-reducing SDS-PAGE followed by lateral transfer onto sheets of nitrocellulose membrane to facilitate detection with biotinylated goat anti-mouse IgG immunoglobulin. Subsequent analysis entailed incubation of nitrocellulose membranes with strepavidin-HRPO in combination with the use of a HRPO chemiluminescent substrate for the acquisition of autoradiography images.

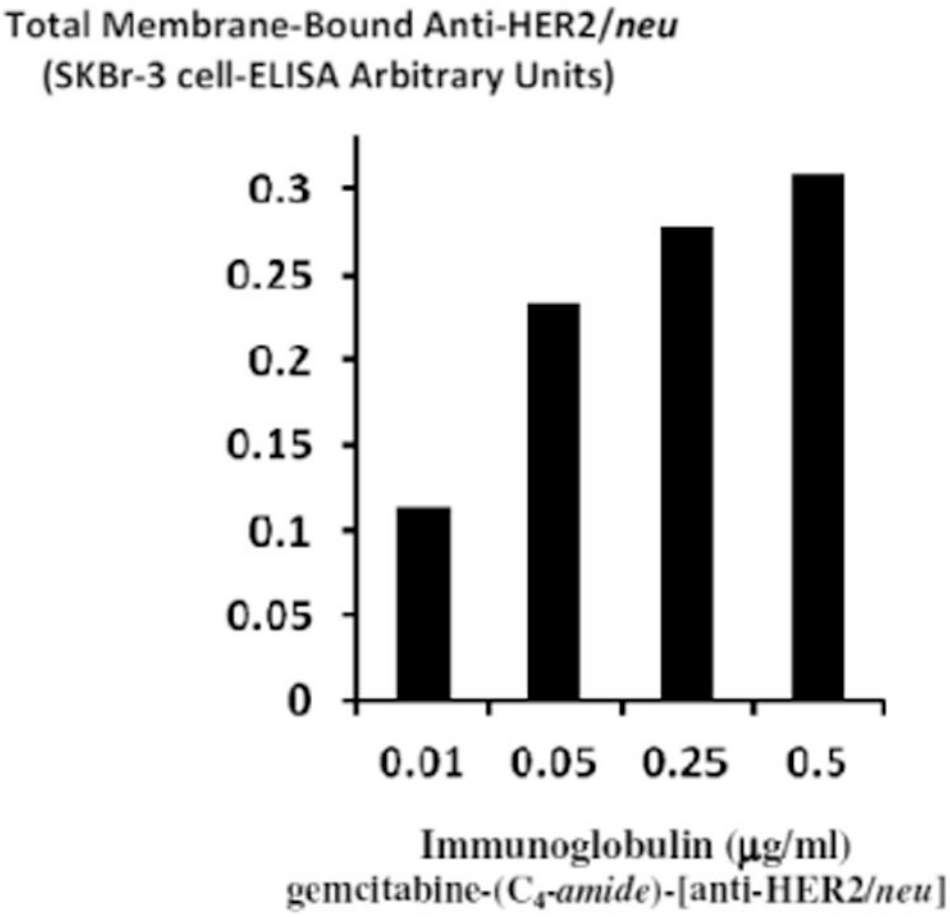

Figure 3.

Detection of total anti-HER2/*neu* immunoglobulin in the form of gemcitabine-(C_4-*amide*)-[anti-HER2/*neu*] bound to the exterior surface membrane of chemotherapeutic-resistant mammary adenocarcinoma (SKBr-3). Covalent gemcitabine-(C_4-*amide*)-[anti-HER2/*neu*] immunochemotherapeutic was incubated with monolayer populations of mammary adenocarcinoma (SKBr-3) over a 4-hour period and total immunoglobulin bound to the exterior surface membrane was measured by cell-ELISA.

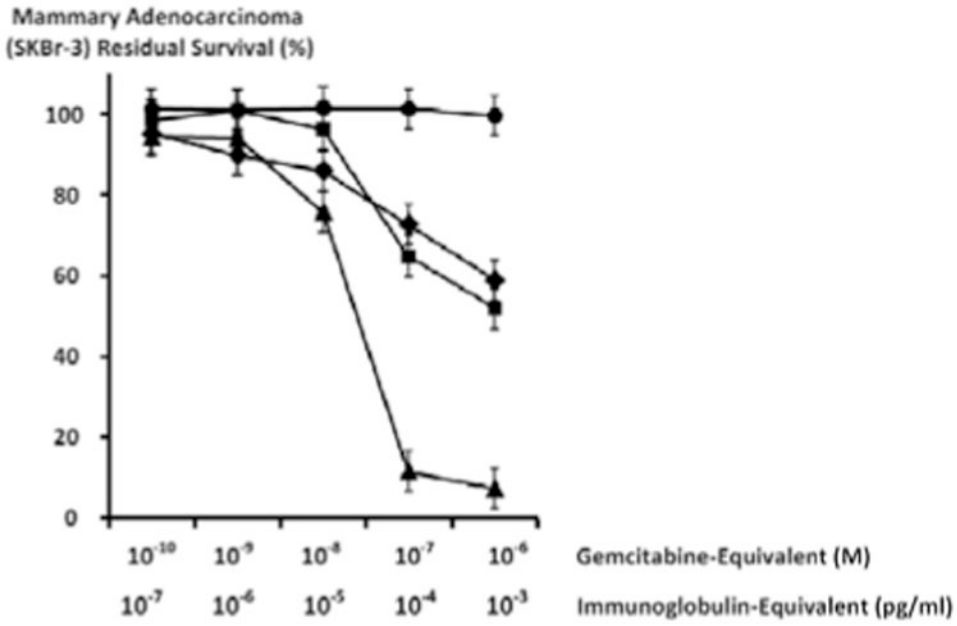

Figure 4.

Differences in cytotoxic anti-neoplastic potency for gemcitabine-(C_4-*amide*)-[anti-HER2/*neu*] compared to gemcitabine alone. *Legends*: (◆) covalent gemcitabine-(C_4-*amide*)-[anti-HER2/*neu*] immunochemotherapeutic following a 182-hours incubation period; (■) gemcitabine chemotherapeutic following a 72-hour incubation period; (▲) gemcitabine chemotherapeutic following a 182-hour incubation period; and (•) anti-HER2/*neu* monoclonal immunoglobulin Chemotherapeutic-resistant mammary adenocarcinoma (SKBr-3) monolayer populations were incubated with covalent gemcitabine-(C_4-*amide*)-[anti-HER2/*neu*] or gemcitabine formulated in triplicate at gradient gemcitabine-equivalent concentrations. Cytotoxic anti-neoplastic potency was measured using a MTT cell vitality assay relative to matched negative reference controls.

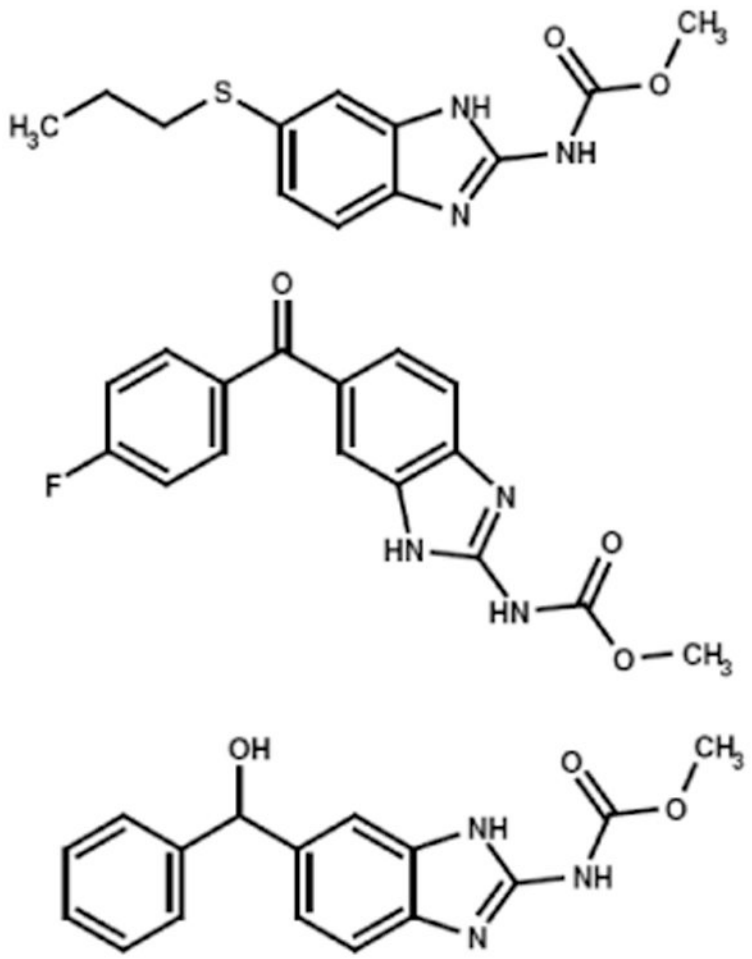

Figure 5.

Molecular structures and chemical composition of representative benzimidazoles evaluated for cytotoxic anti-neoplastic potency against chemotherapeutic-resistant mammary adenocarcinoma (SKBr-3) populations. *Legends*: (*Top*) albendazole, (*Middle*) flubendazole, and (*Bottom*) mebendazole.

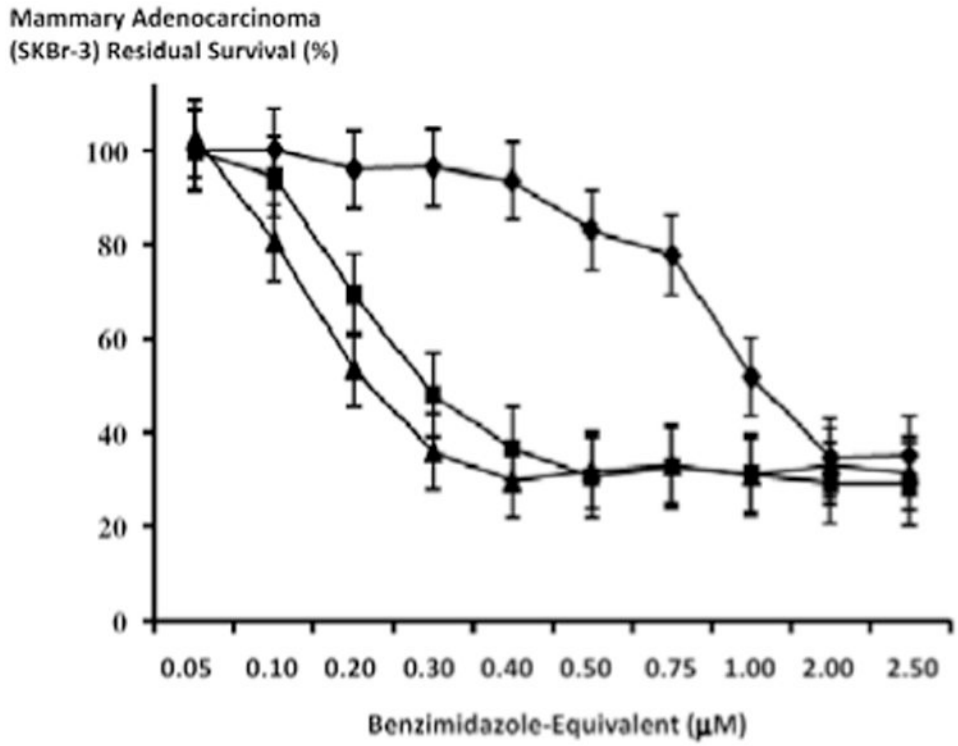

Figure 6.

Relative cytotoxic anti-neoplastic potency of benzimidazoles against chemotherapeutic-resistant human mammary adenocarcinoma. *Legend*: (◆) albendazole; (▲) flubendazole; and (■) mebendazole. Chemotherapeutic-resistant mammary adenocarcinoma (SKBr-3) monolayer populations were incubated for 72-hours with the benzimidazole tubulin/microtubule inhibitors formulated in triplicate at gradient molar-equivalent concentrations. Cytotoxic anti-neoplastic potency was measured using a MTT cell vitality assay relative to matched negative reference controls.

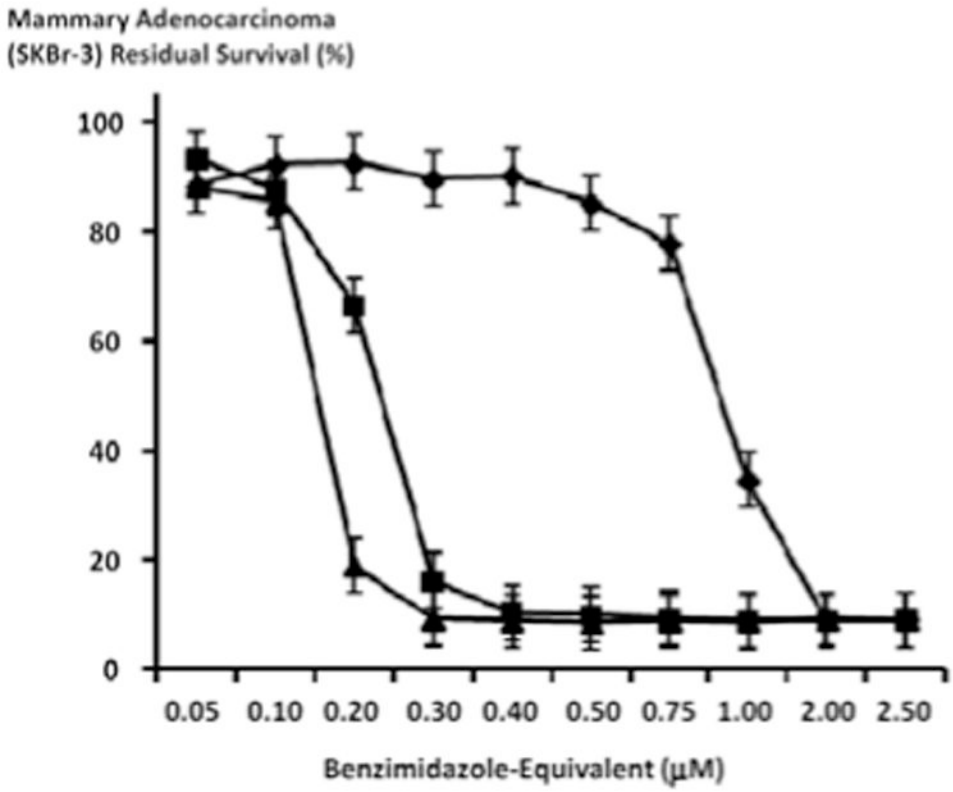

Figure 7.

Relative cytotoxic anti-neoplastic potency of benzimidazoles against chemotherapeutic-resistant mammary adenocarcinoma (SKBr-3). *Legends*: (◆) albendazole; (▲) flubendazole; and (■) mebendazole. Chemotherapeutic-resistant mammary adenocarcinoma (SKBr-3) monolayer populations were incubated for 182-hours with the benzimidazole tubulin/microtubule inhibitors formulated in triplicate at gradient molar-equivalent concentrations. Cytotoxic anti-neoplastic potency was measured using a MTT cell vitality assay relative to matched negative reference controls.

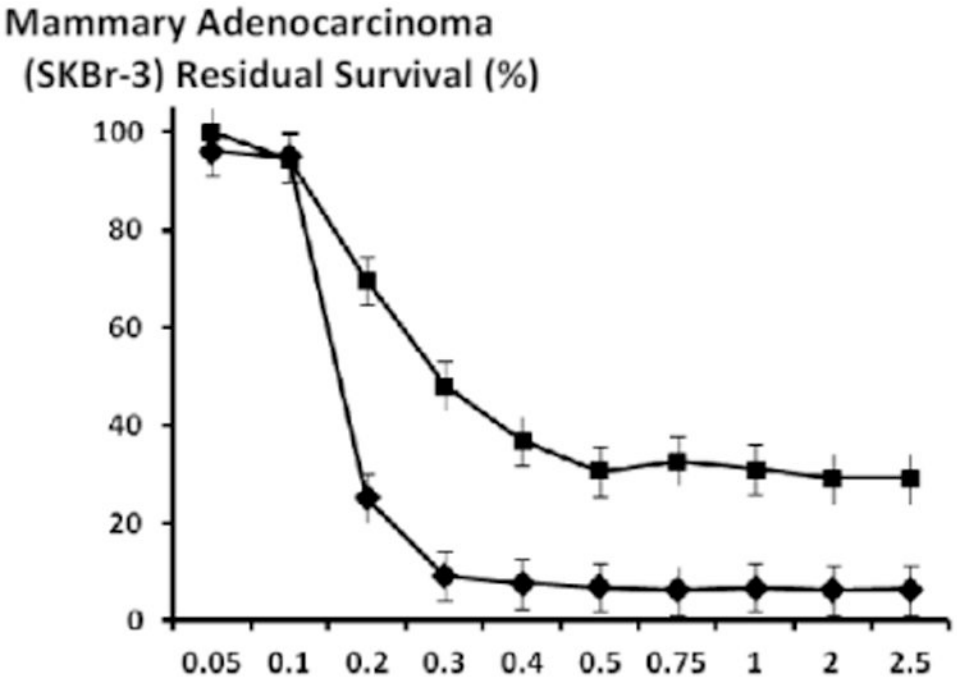

Figure 8.

Relative cytotoxic anti-neoplastic potency of benzimidazoles against chemotherapeutic-resistant mammary adenocarcinoma (SKBr-3). *Legends*: (◆) albendazole; (▲) flubendazole; and (■) mebendazole. Chemotherapeutic-resistant mammary adenocarcinoma (SKBr-3) monolayer populations were incubated for 182-hours with the benzimidazole tubulin/microtubule inhibitors formulated in triplicate at gradient molar-equivalent concentrations. Cytotoxic anti-neoplastic potency was measured using a MTT cell vitality assay relative to matched negative reference controls.

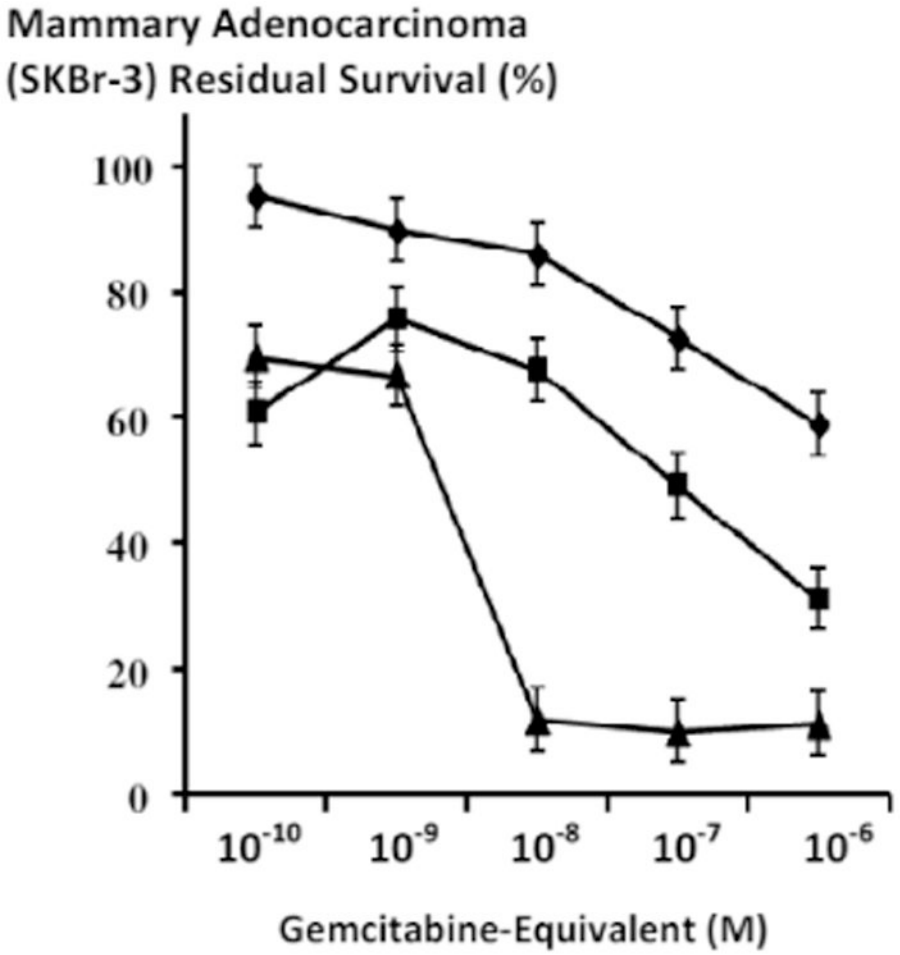

Figure 9.

Influence on the cytotoxic anti-neoplastic potency of gemcitabine-(C_4-*amide*)-[anti-HER2/*neu*] when applied in dual combination with mebendazole against chemotherapeutic-resistant human mammary adenocarcinoma. *Legends*: (■) covalent gemcitabine-(C_4-*amide*)-[anti-HER2/*neu*] immunochemotherapeutic and mebendazole; (◆) covalent gemcitabine-(C_4-*amide*)-[anti-HER2/*neu*] immunochemotherapeutic; and (▲) gemcitabine with mebendazole Chemotherapeutic-resistant mammary adenocarcinoma (SKBr-3) monolayer populations were incubated with gemcitabine-(C_4-*amide*)-[anti-HER2/*neu*] formulated in triplicate at gradient concentrations (+/- mebendazole 0.15 μM fixed-concentration). Cytotoxic anti-neoplastic potency was measured using a MTT cell vitality assay relative to matched negative reference controls.

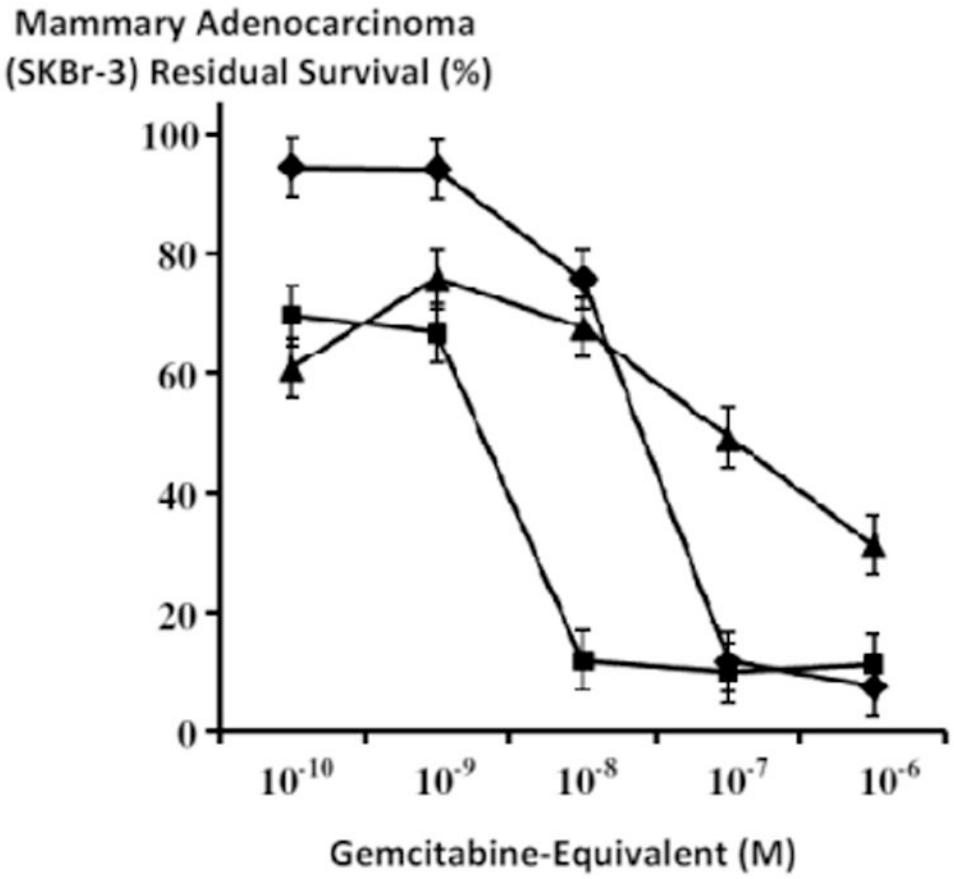

Figure 10.

Relative cytotoxic anti-neoplastic potency of gemcitabine-(C_4-*amide*)-[anti-HER2/*neu*] in combination with mebendazole compared to gemcitabine against chemotherapeutic-resistant human mammary adenocarcinoma. Legend: (▲) gemcitabine-(C_4-*amide*)-[anti-HER2/*neu*] with mebendazole; (■) gemcitabine with mebendazole; and (◆) gemcitabine without mebendazole. Chemotherapeutic-resistant mammary adenocarcinoma (SKBr-3) monolayer populations were incubated 182 hours with gemcitabine-(C_4-*amide*)-[anti-HER2/*neu*] in combination with mebendazole (0.15 μM fixed-concentration), or gemcitabine alone each formulated in triplicate at gradient gemcitabine-equivalent concentrations. Cytotoxic anti-neoplastic potency was measured using a MTT cell vitality assay relative to matched negative reference controls.